

Dynamics and fragmentation in Galactic filamentary structures

Sandra Patricia Treviño-Morales

Treviño-Morales S. P., Pilleri P., Fuente A., et al. 2014, A&A, 569, A19

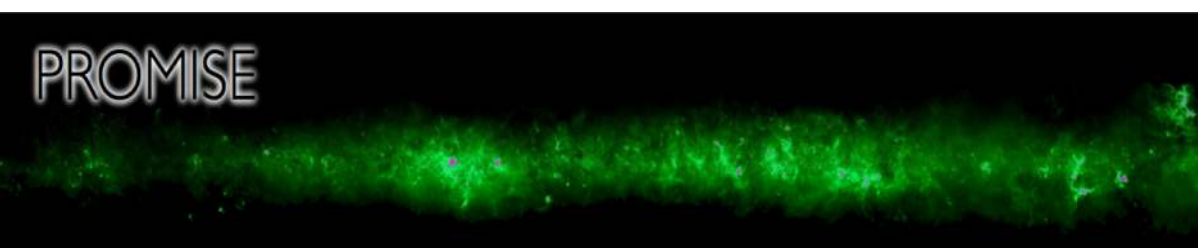
Treviño-Morales S. P., Fuente A., Sánchez-Monge Á., et al. 2016, A&A, 593, 139 L12 140

Kainulainen J., Stutz A. M., Stanke T., et al. 2017, A&A, 600, A141

Treviño-Morales S. P., Fuente A., Sánchez-Monge A., et al. 2019, A&A, arXiv:1907.03524

Treviño-Morales S. P., Kainulainen J., Orkisz J., et al. 2019, A&A, in prep.

Laboratoire AIM, CEA/IRFU/SAp - CNRS - Université Paris Diderot, Paris-Saclay, September, 2019



PROMISE



CHALMERS
UNIVERSITY OF TECHNOLOGY



PRobing the Origins of Massive molecular cloud StructurE



Manuel Riener

PhD student at MPIA

Physical process controlling star formation in molecular clouds; star formation in nearby galaxies



Jouni Kainulainen

Assistant professor at Chalmers

Observational astronomer in the field of Galactic star formation and interstellar medium

Miaomiao Zhang

Postdoc at MPIA

Young stellar objects; jets and outflows, Galactic star formation and ISM



Andri Spilker

PhD student at Chalmers

Molecular cloud structure, star formation in the Milky Way



Sara Rezaeikhoshbakht

Postdoc at Chalmers

3D distribution of dust in the Milky Way Galaxy



Jan Orkisz

Postdoc at Chalmers

ISM turbulence and magnetic fields, star formation

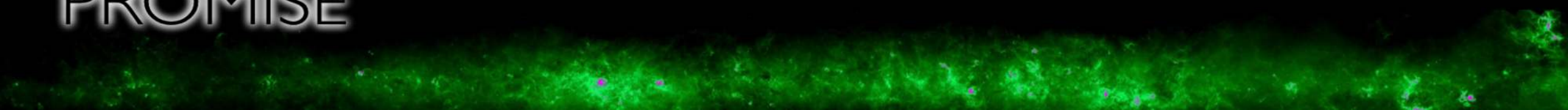


Sandra Treviño-Morales

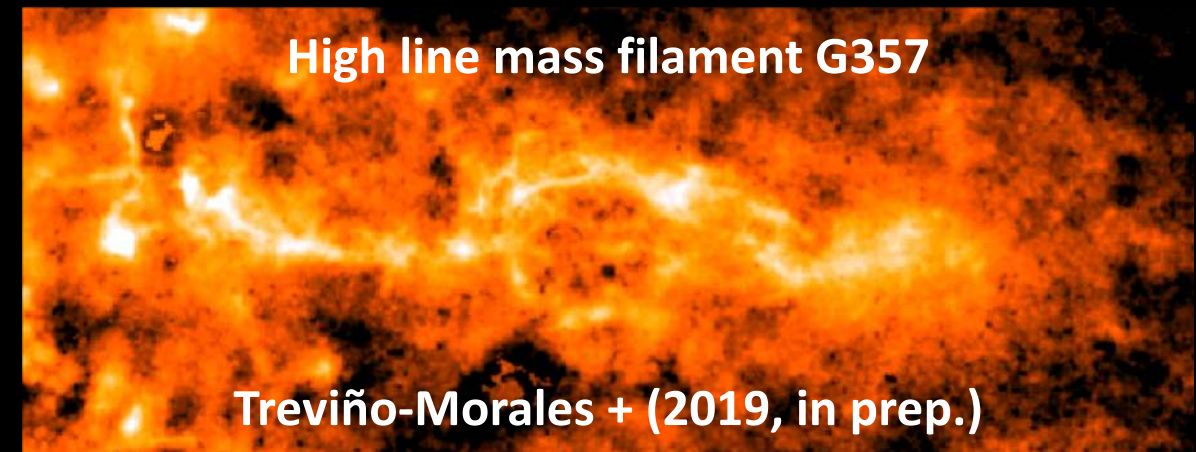
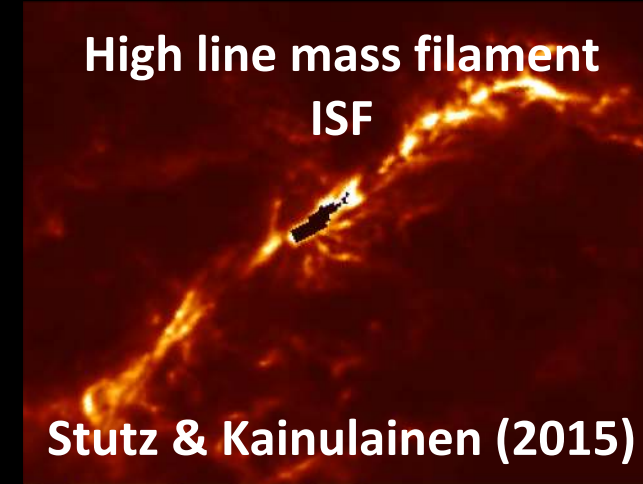
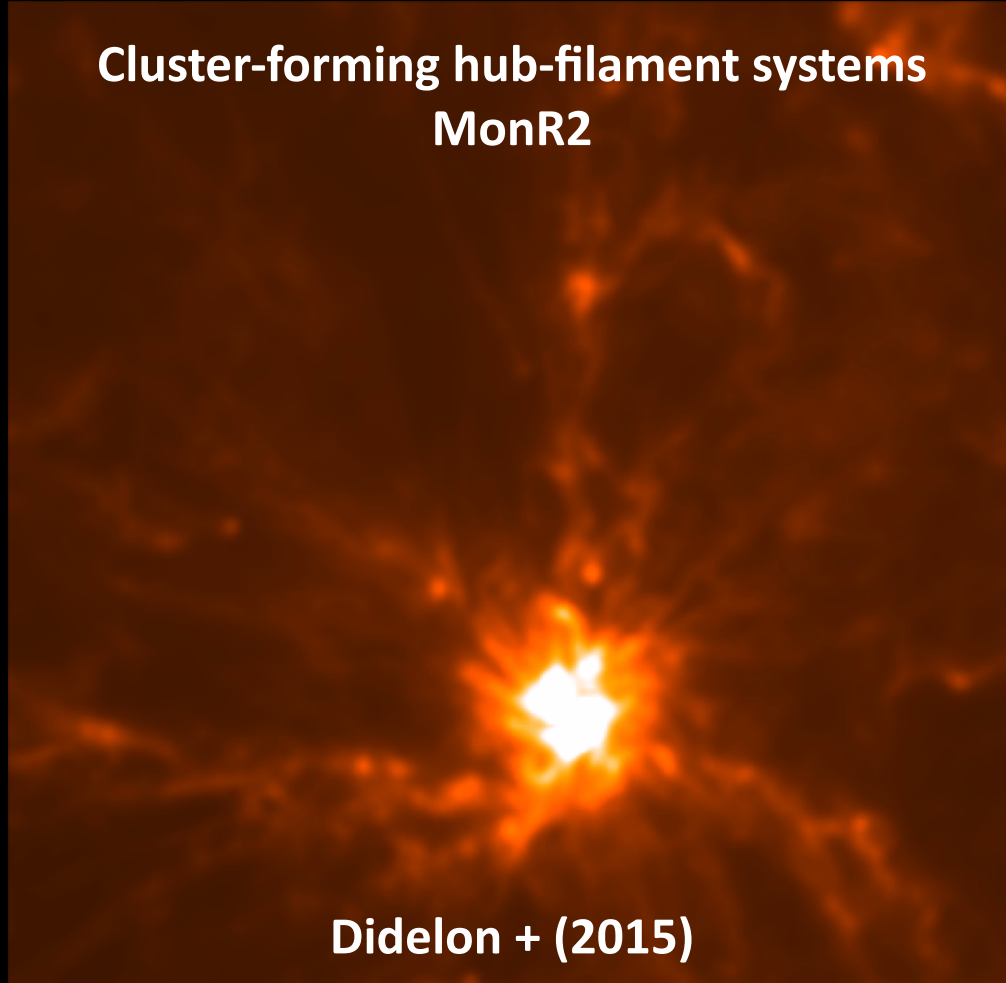
Postdoc at Chalmers

Dynamics and fragmentation in Galactic molecular clouds, astrochemistry in HII and PDR

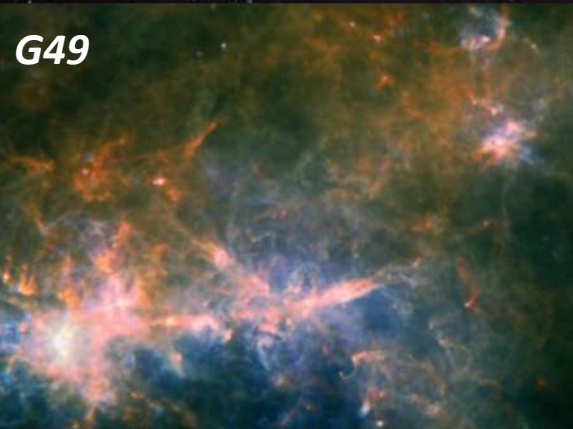
PROMISE



Study of dynamics and fragmentation in filamentary structures



Filaments permeate the ISM on all scales



G49
ESA/Herschel/PACS/SPIRE/Keck
Wang et al. 2015



Orion A
ESA/Herschel/André, Polychroni, Roy,
Könyves, Schneider: Gould Belt
survey Key Program



Rosetta
ESA/Herschel/PACS/SPIRE
HOBYS Key Program Consortia

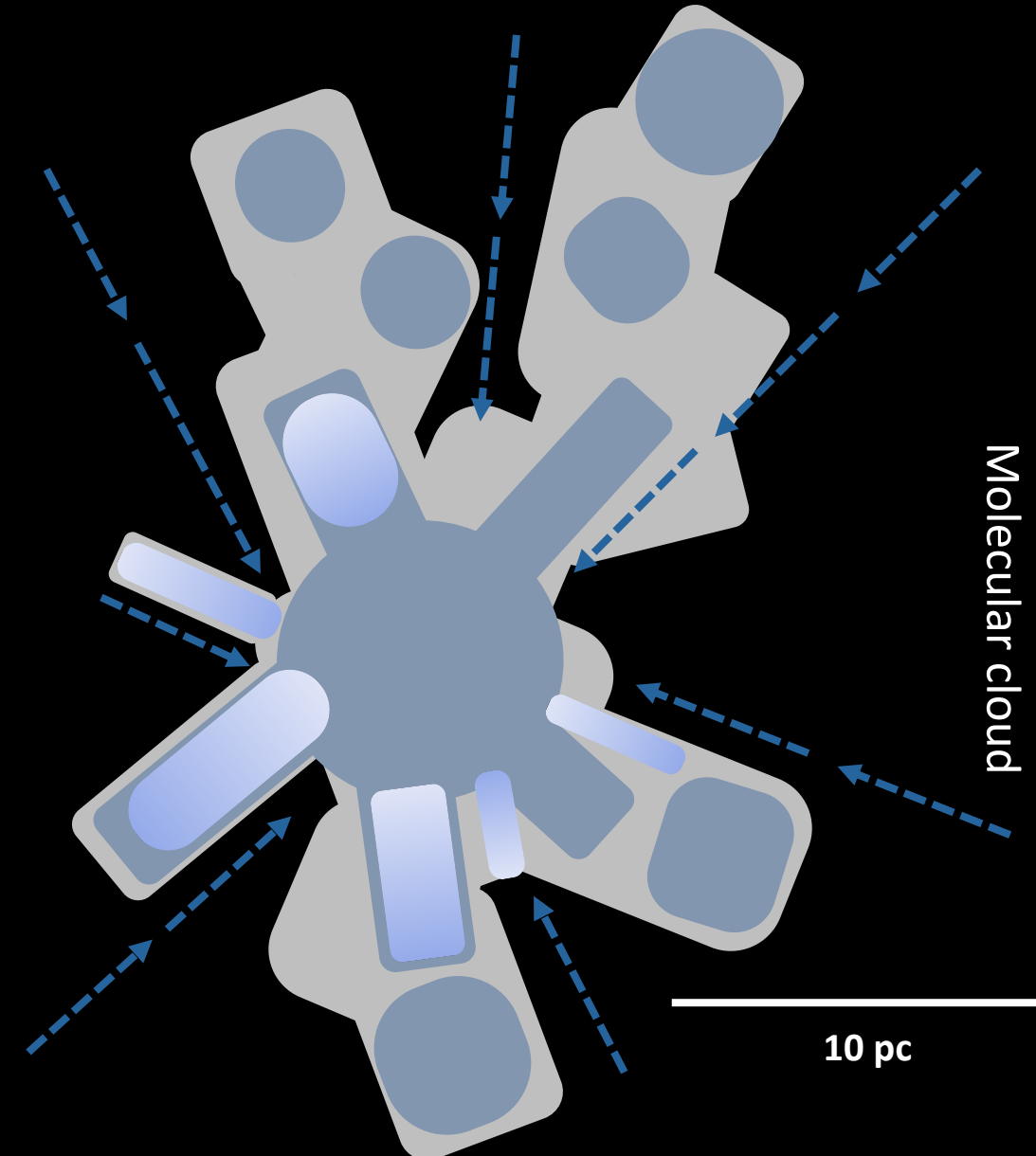
Andre et al. (2010), Molinari et al. (2010), Schneider et al. (2010), Csaengeri et al. (2011), Schneider et al. (2012), Hennemann et al. (2012), Busquet et al. (2013), Hacar et al. (2013), Peretto et al. (2014), Louvet et al. (2014), Tafalla & Hacar (2015), Smith et al. (2014), Henshaw et al. (2014), Tackenberg et al. (2014), Seifried & Walch (2015), Hacar et al. (2018), Arzoumanian et al. (2018), Suri et al. (2019), Trevino-Morales et al. (2019) ...

The birthplaces of the stars

Molecular clouds formed by complex networks of filaments intersecting in high-density regions called hub

Unstable against radial collapse and fragmentation ([Inutsuka & Miyama 1997](#)). Their origin or formation process still unclear. However, turbulence, gravity ([Klessen + 2000](#)) and magnetic fields ([Molina + 2012; Kirk + 2015](#)), can produce the observed structures.

Figure adapted from [Baobab \(2010\)](#)



The birthplaces of the stars

Transport of gas along the filaments

$$M = \frac{N}{X} A(2.8 m_H),$$

N = total column density of the molecule

X = relative abundance with respect to H₂

m_H = hydrogen atom mass

$$\dot{M}_{\text{acc}} = \frac{\left(\frac{M}{L_{\text{obs}}} V_{\parallel, \text{obs}}\right)}{\tan(\alpha)} = \frac{M \nabla V_{\parallel, \text{obs}}}{\tan(\alpha)}.$$

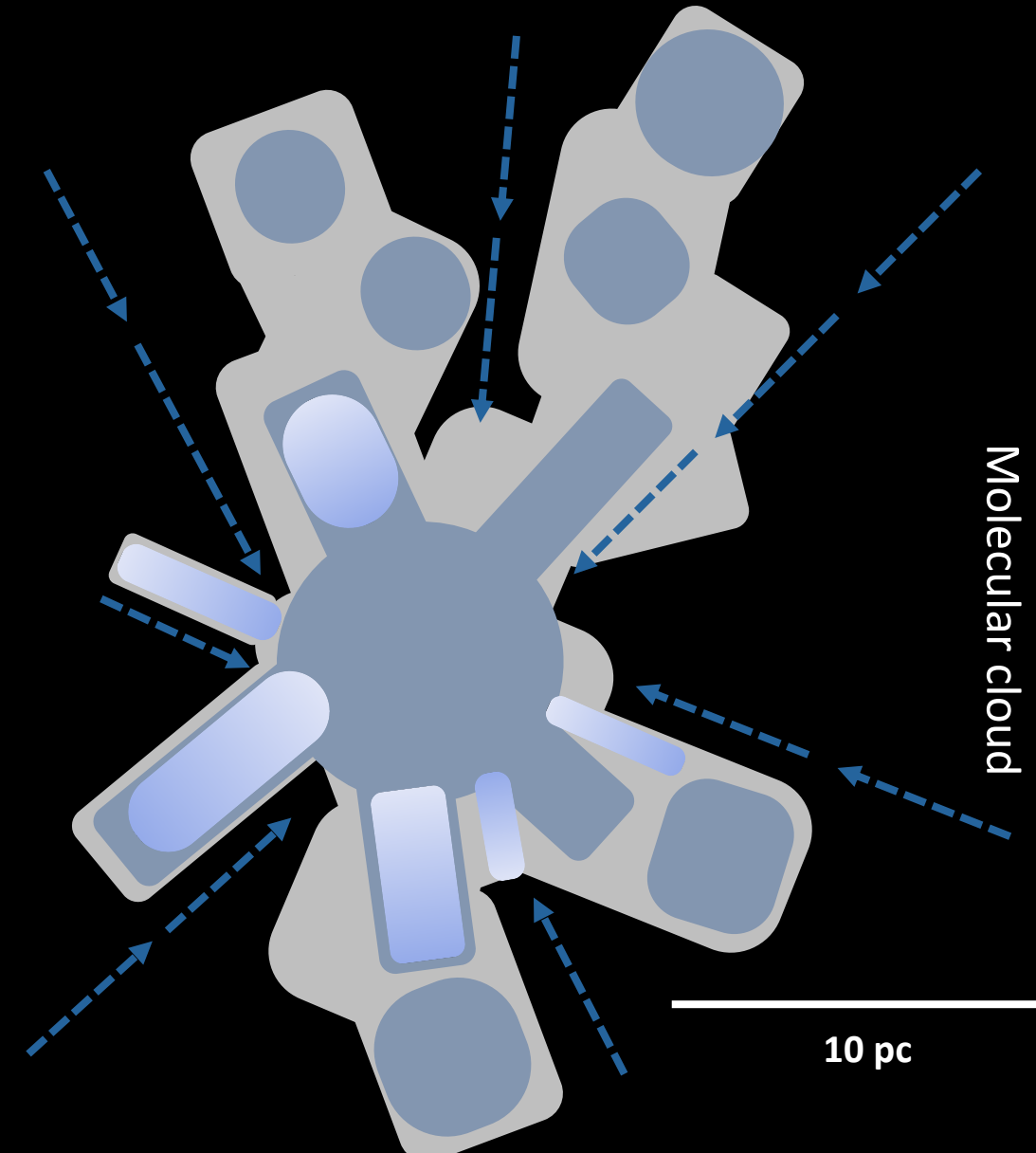
M = filament mass

$\nabla V_{\parallel, \text{obs}}$ = velocity gradient = $V_{\parallel, \text{obs}}/L_{\text{obs}}$

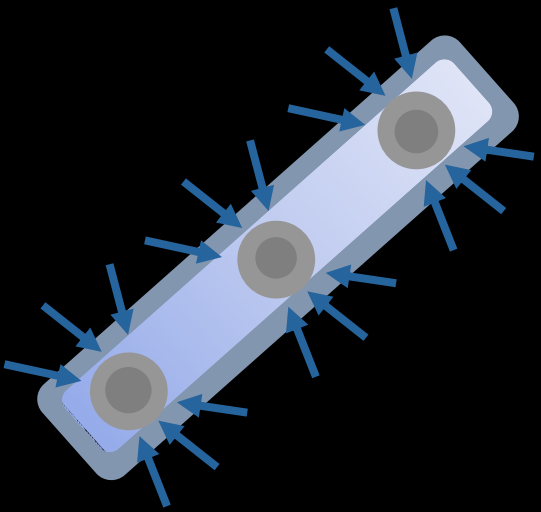
Where $L_{\text{obs}} = L \cos(\alpha)$ and $V_{\parallel, \text{obs}} = V_{\parallel} \sin(\alpha)$

Nagasawa (1987); Kirk + (2013); Wang + (2014)

Figure adapted from Baobab (2010)



The birthplaces of the stars

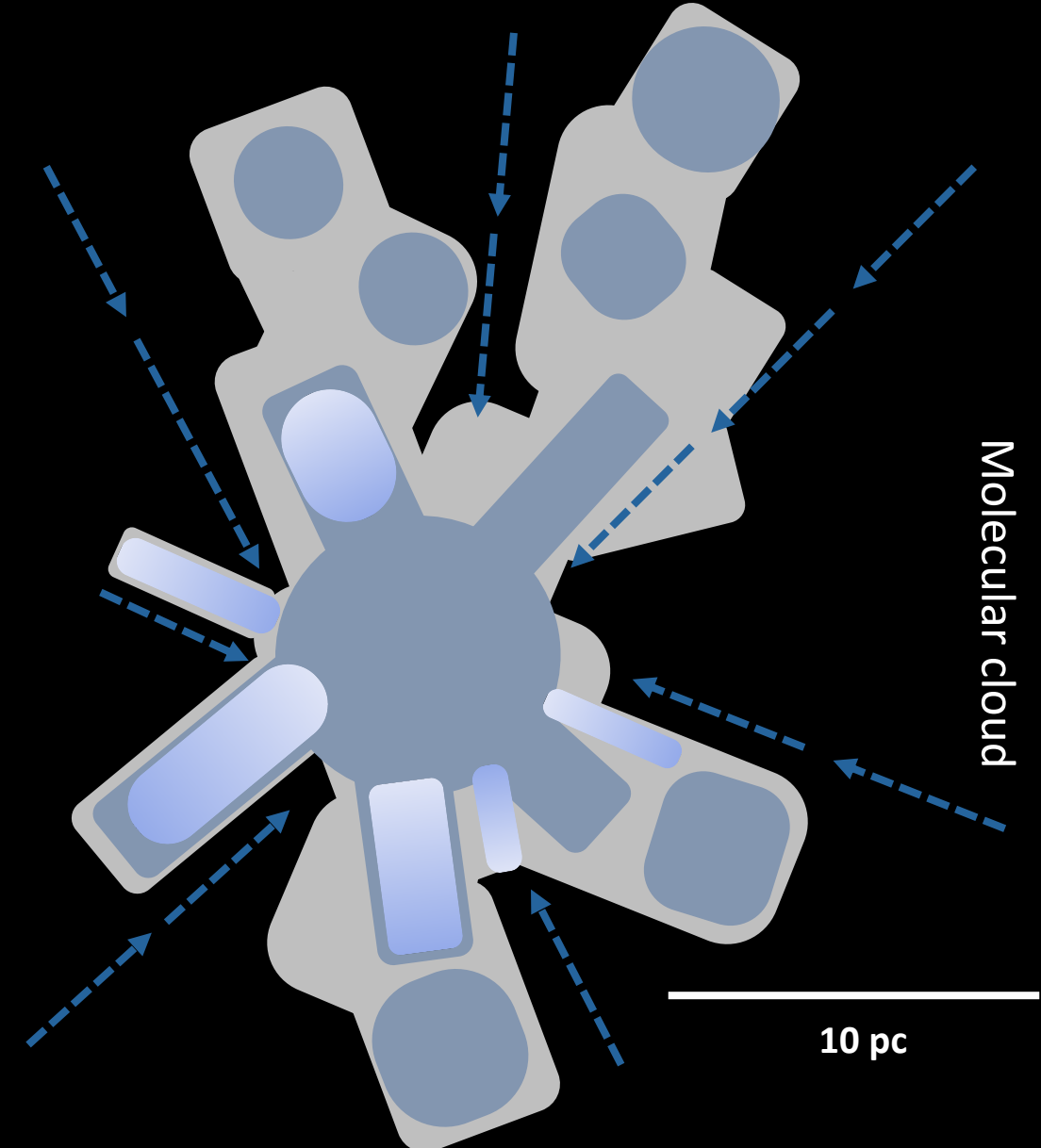


$$M_{\text{line}} = M/L$$

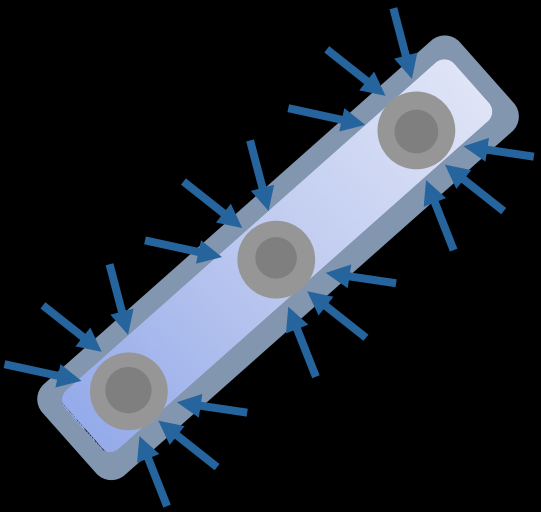
In the case of an **isolated, infinitely long filament** where **gravity and thermal pressure** are the only forces, an equilibrium solution exists at the

$$(M/L)_{\text{crit},064} = \frac{2c_s^2}{G} = 16.7 \left(\frac{T}{10 \text{ K}} \right) M_{\odot} \text{ pc}^{-1},$$

Figure adapted from Baobab (2010)



The birthplaces of the stars



$$M_{\text{line}} = M/L$$

$$(M/L)_{\text{crit},064} = \frac{2c_s^2}{G} = 16.7 \left(\frac{T}{10 \text{ K}} \right) M_{\odot} \text{ pc}^{-1},$$

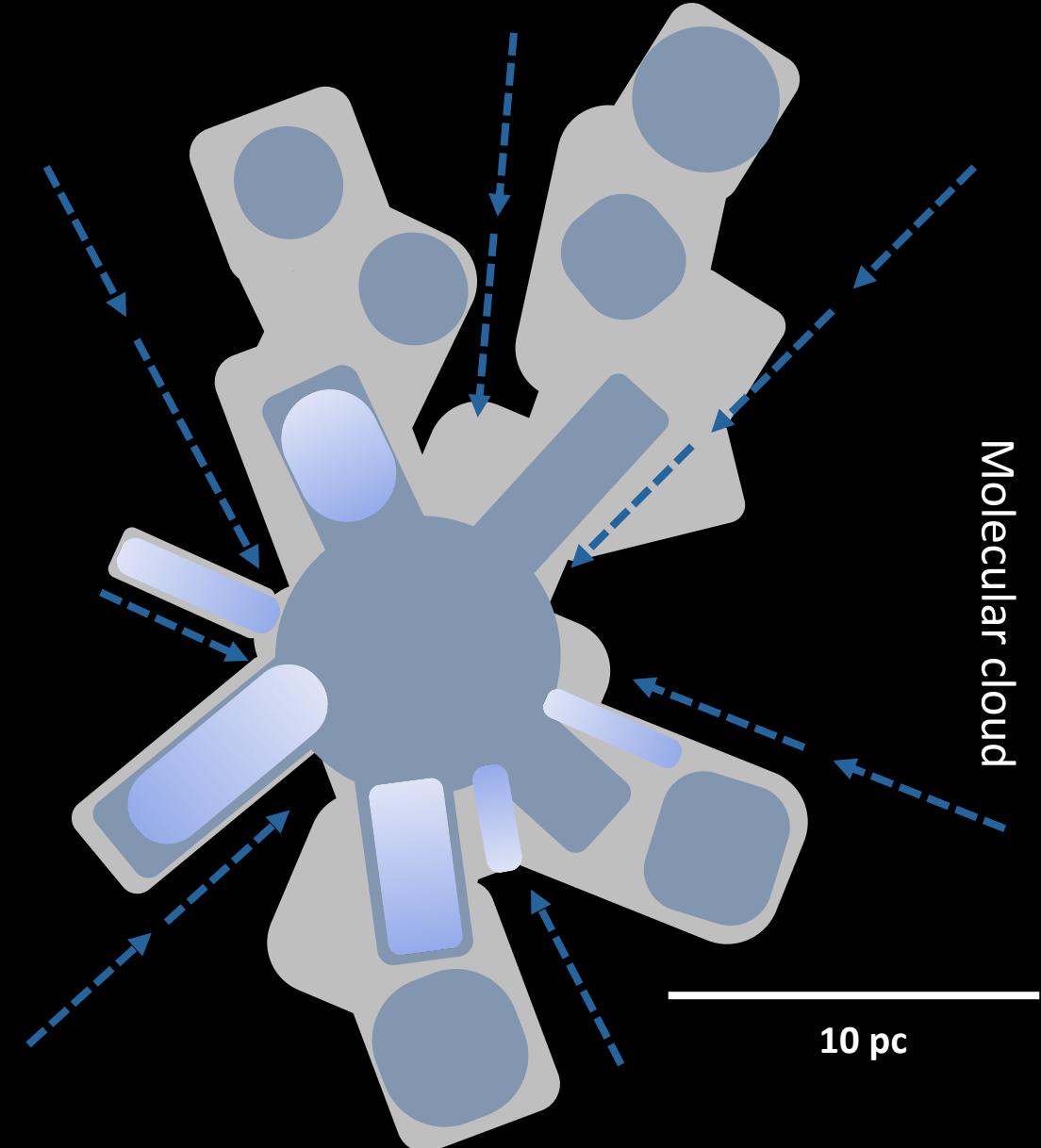
c_s = sound speed = $(kT/\mu m_H)^{1/2}$

G = gravitational constant.

T = temperature.

Ostriker 1964; Inutsuka & Miyama 1997

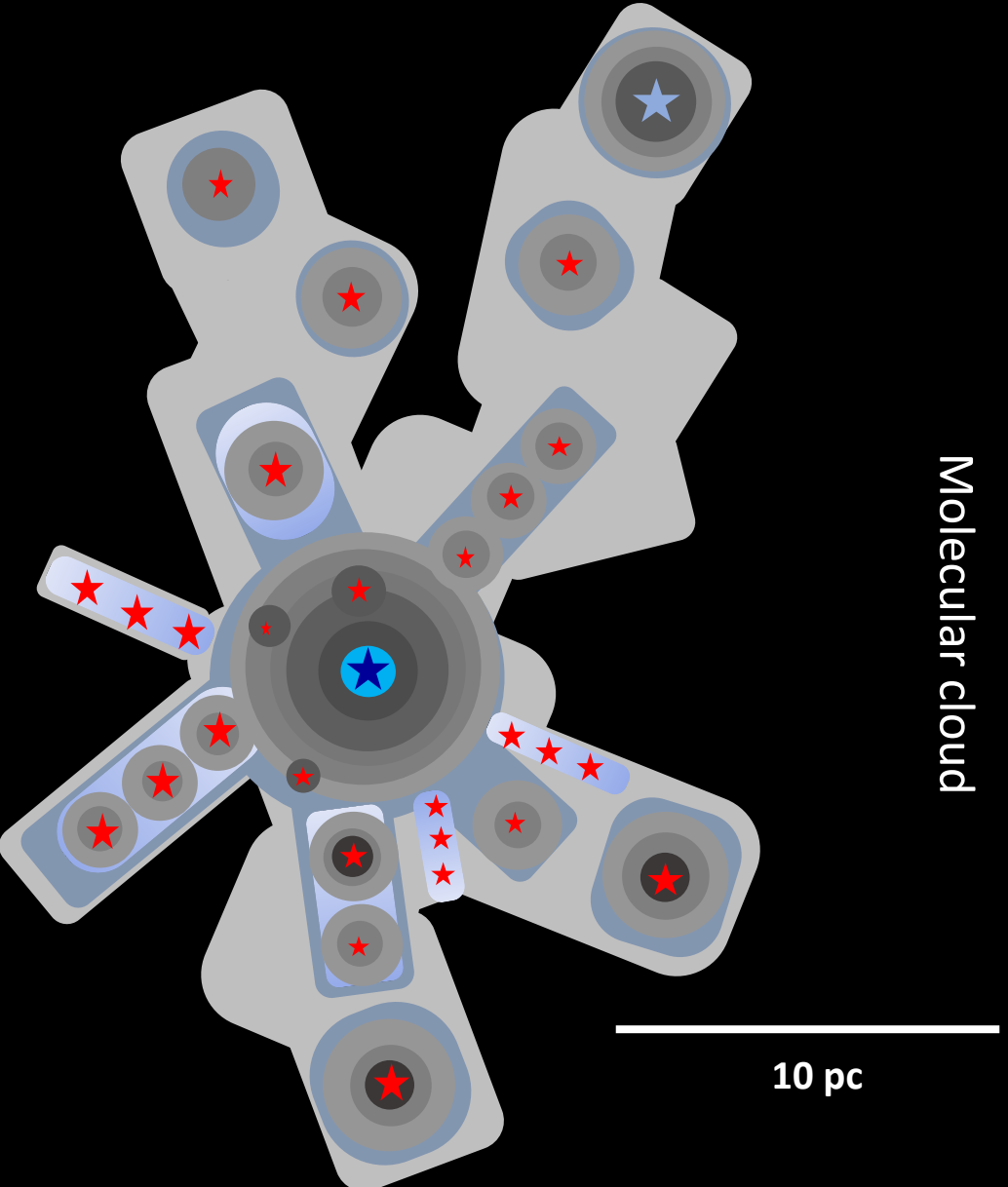
Figure adapted from Baobab (2010)



The birthplaces of the stars

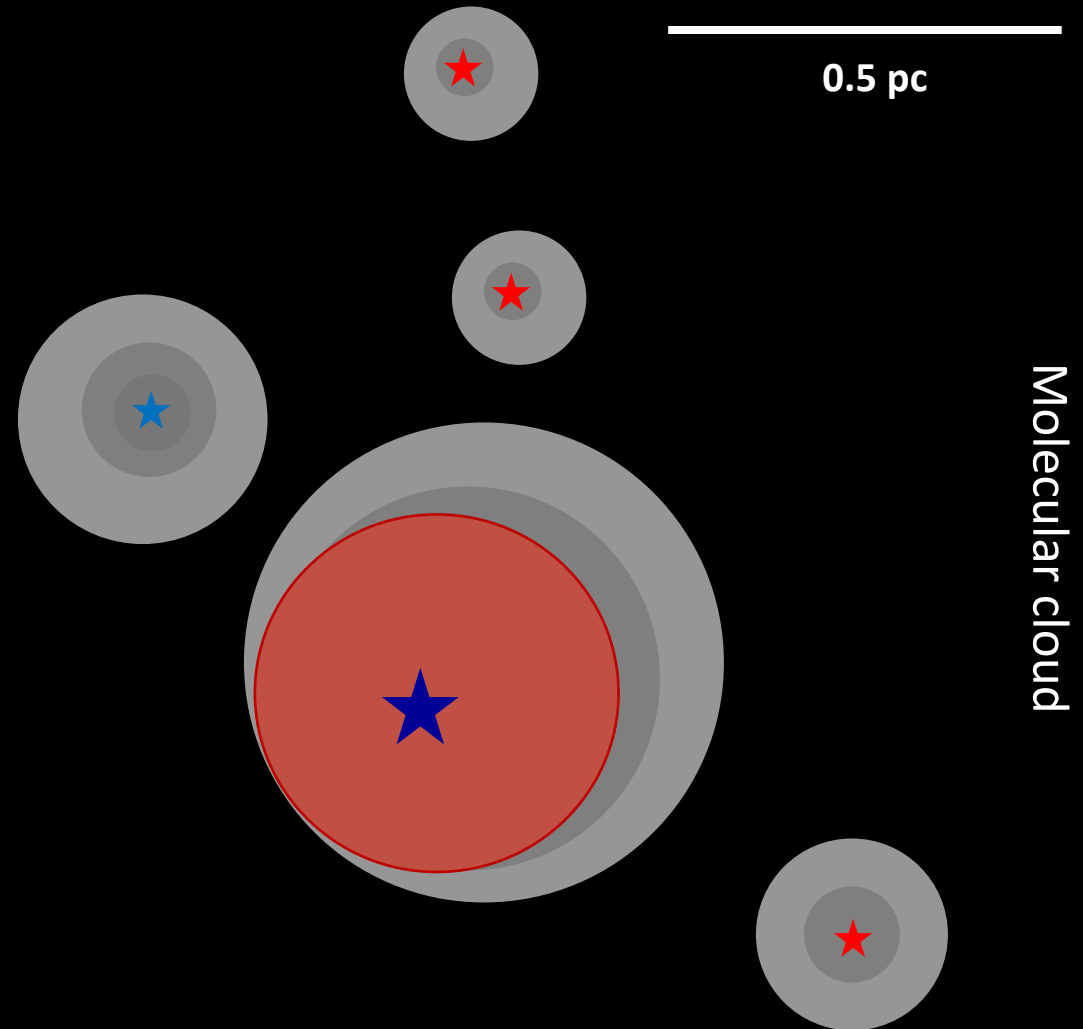
Star formation occurs along the filaments
High-mass stars forming at the hubs

Figure adapted from Baobab (2010)



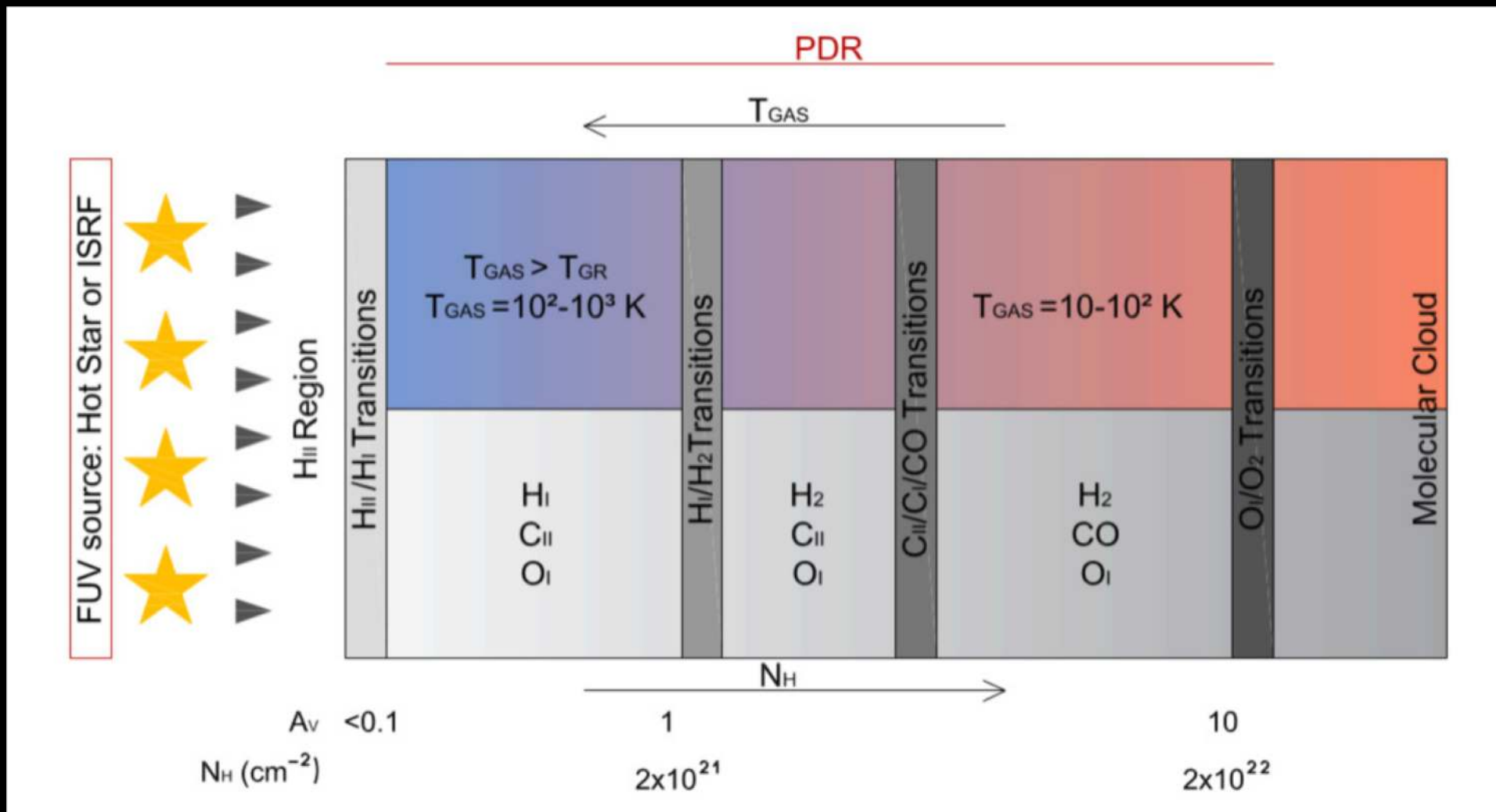
Massive star effects: HII region and Photon-Dominated Region system

A massive star (O & B type) radiates enough **UV photons** with **energies $E > 13.6 \text{ eV}$** that ionize the surrounding gas and generate an **HII régión** ... radiates **photons** with energies $6 < E < 13.6 \text{ eV}$ that **dissociate H_2** and **CO** molecules and generate a **PDR**.



Link between HII region and molecular cloud

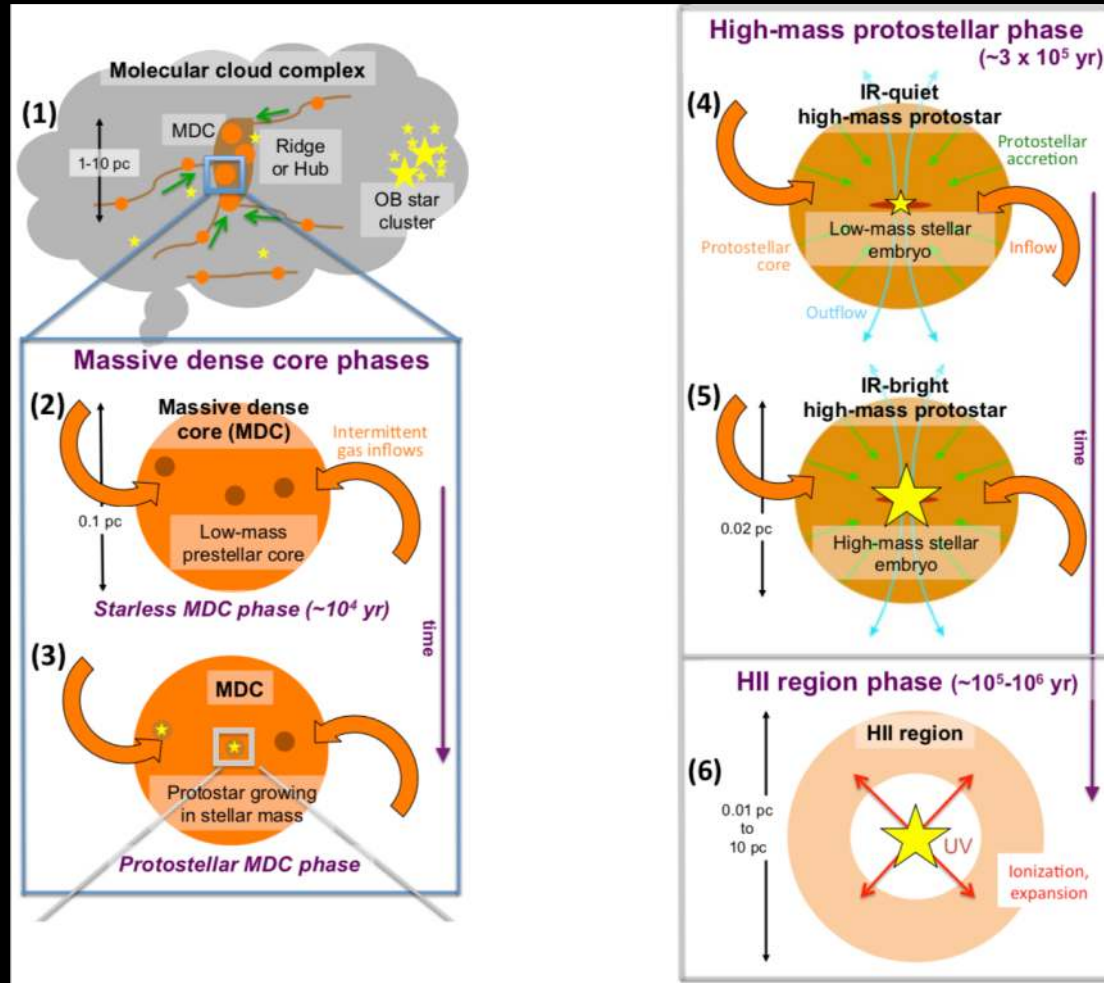
What is a Photon-Dominated Region (PDR)?



Adapted from Hollenbach & Tielens (1997)

Schematic evolutionary diagram proposed for massive stars formation

Motte + (2018)



Massive stellar clusters form in extreme clouds called ridges. Unlike the case of low-mass stars which accrete their final mass from well-defined pre-stellar cores, with a mass distribution mimicking the IMF ([Motte +1998; Könyves + 2015](#)), high-mass stars within ridges should have a complex accretion history.

One should therefore investigate the detailed properties cluster-forming hub-filament system and ridges to constrain the outcome characteristics of massive clusters.

Alzirr

Where can we study this kind of structures?

Altarf

Gomeisa

NGC 2264

Meissa

Procyon

MONOCEROS

ζ Mon
M 48

α Mon

δ Mon

IC 2177

M 46

M 47

Sirius

18 Mon

β Mon

γ Mon

13 Mon

8 Mon

Nebulosa Rosetta

Betelgeuse

Bellatrix

Mintaka

Alnilam
Alnitak

IC 434

M 42

IC 2118

Saiph

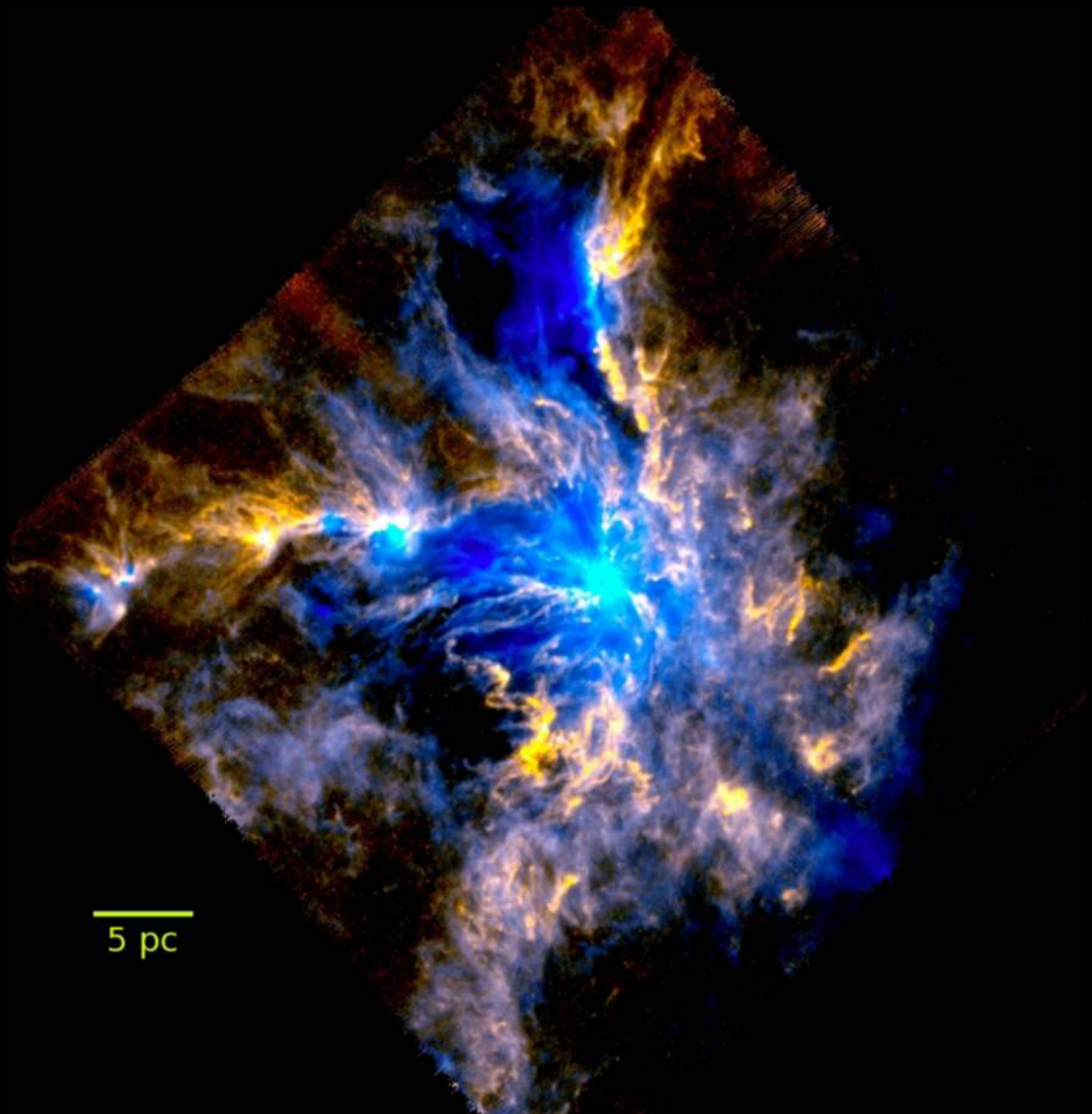
Rigel

Cinturon
de Barnard



Monoceros R2 molecular cloud

Pokhrel + (2016)



The **Monoceros molecular cloud** (at 830 pc) contains several sites of active star formation

Estimated the mass of $4 \times 10^4 M_{\odot}$ in an area of 44pc \times 55pc.

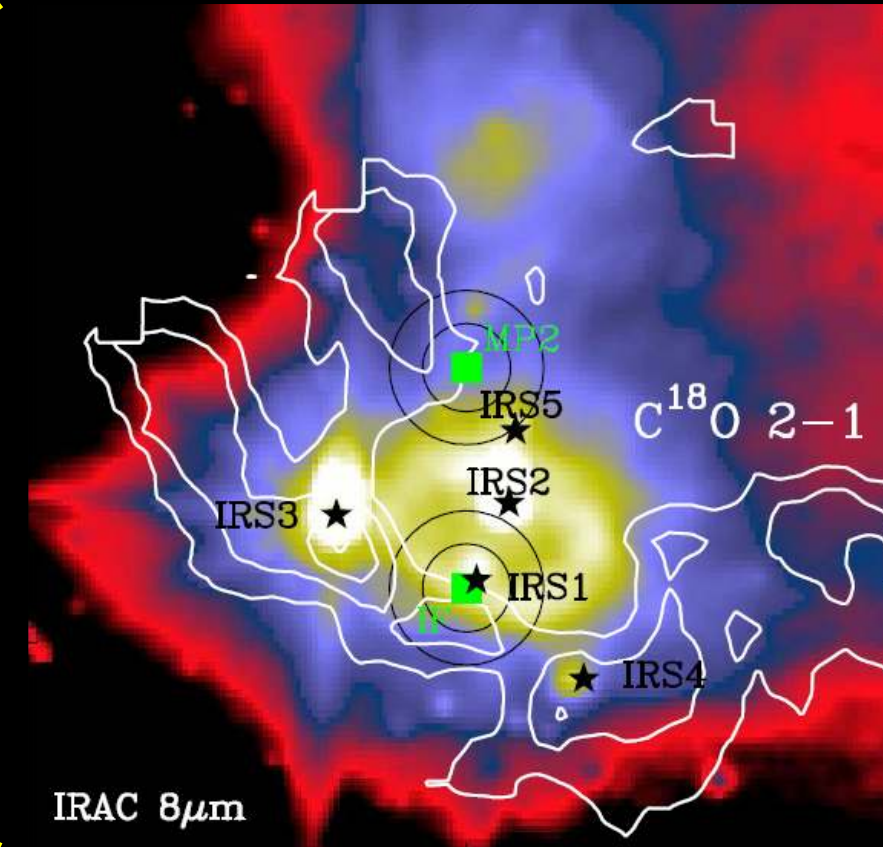
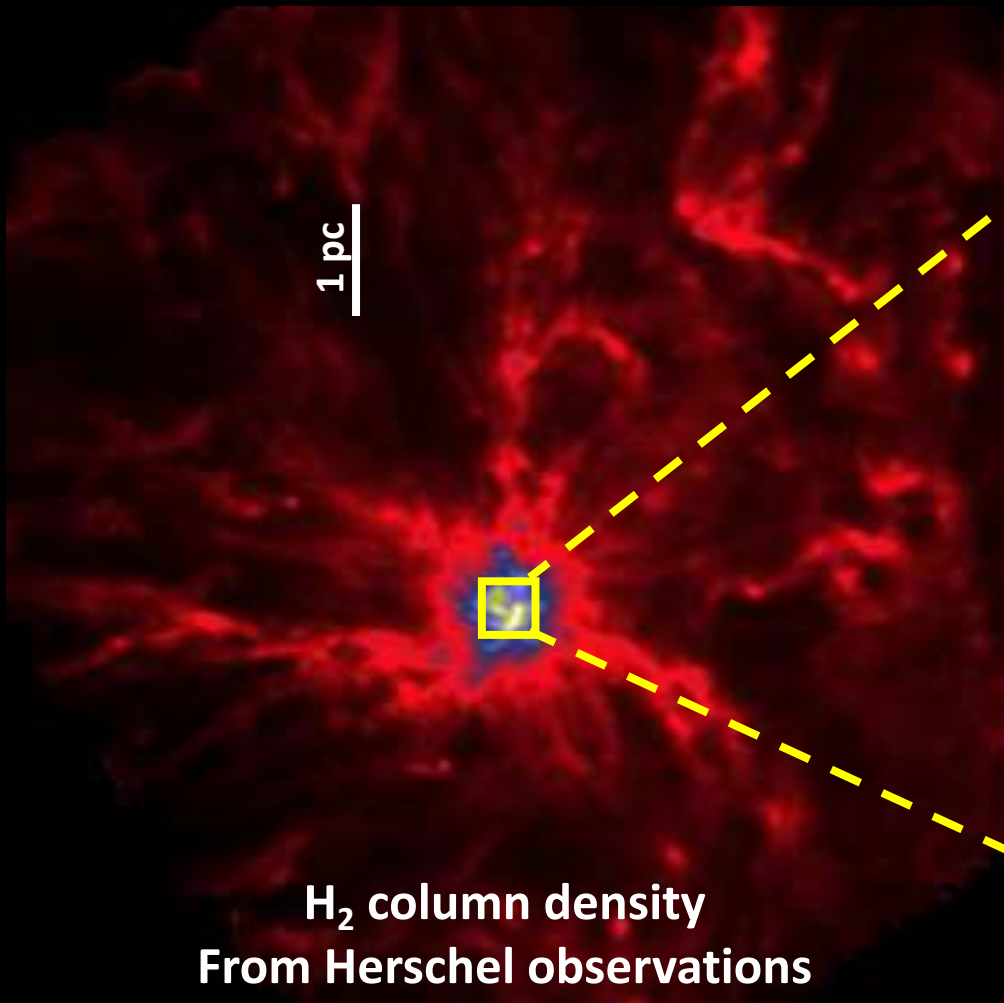
- **Mon R2** is the most massive and prominent cluster

- ... rich cluster with 371 objects, including massive (**B-type**) stars
 - ... large mass reservoir, with a total mass of $\sim 10\,000 M_{\odot}$

Miesch, Scalo & Bally (1999); Xie (1992); Carpenter (2000); Carpenter & Hodapp (2008)

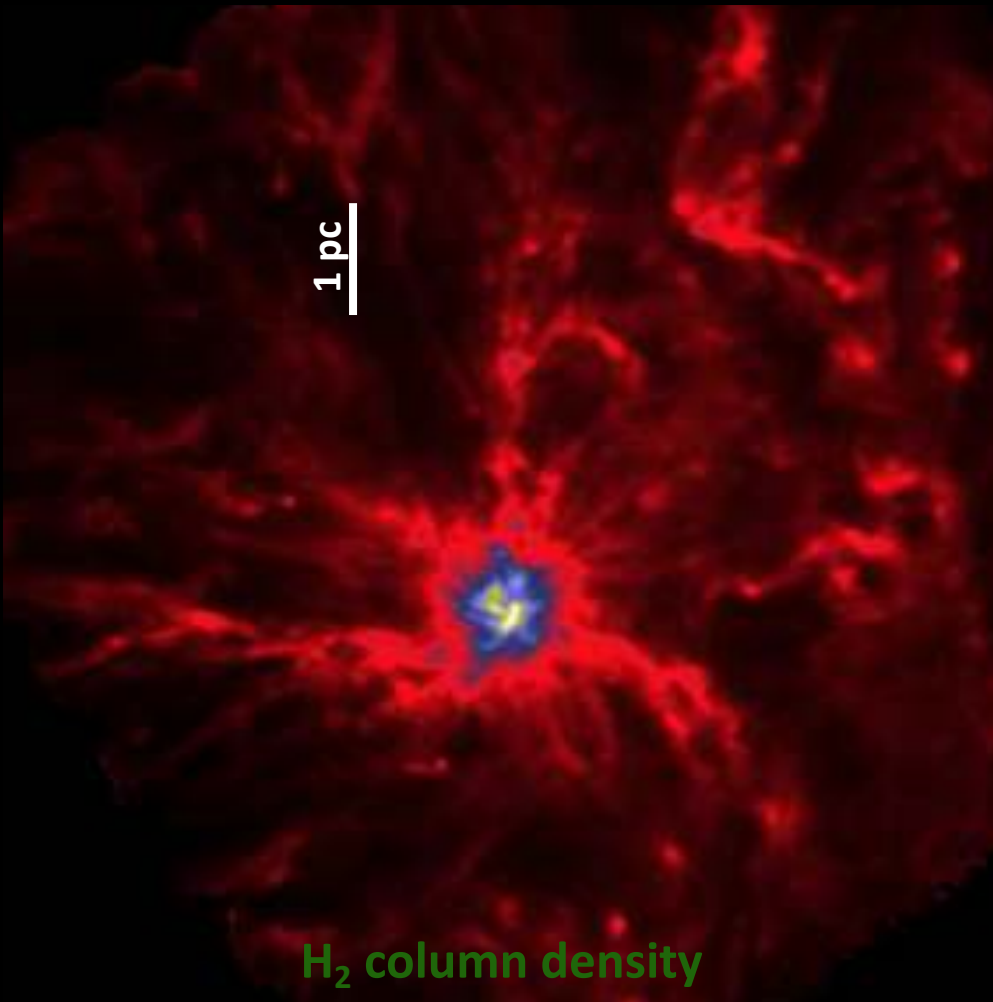
Monoceros R2 molecular cloud

Didelon + (2015)



Monoceros R2 molecular cloud

Didelon + (2015)



Cluster-forming hub-filament system

UC H_{II} region

PDRs with different conditions

Is an excellent target to study

- kinematics,
- dynamics,
- feedback
- chemistry

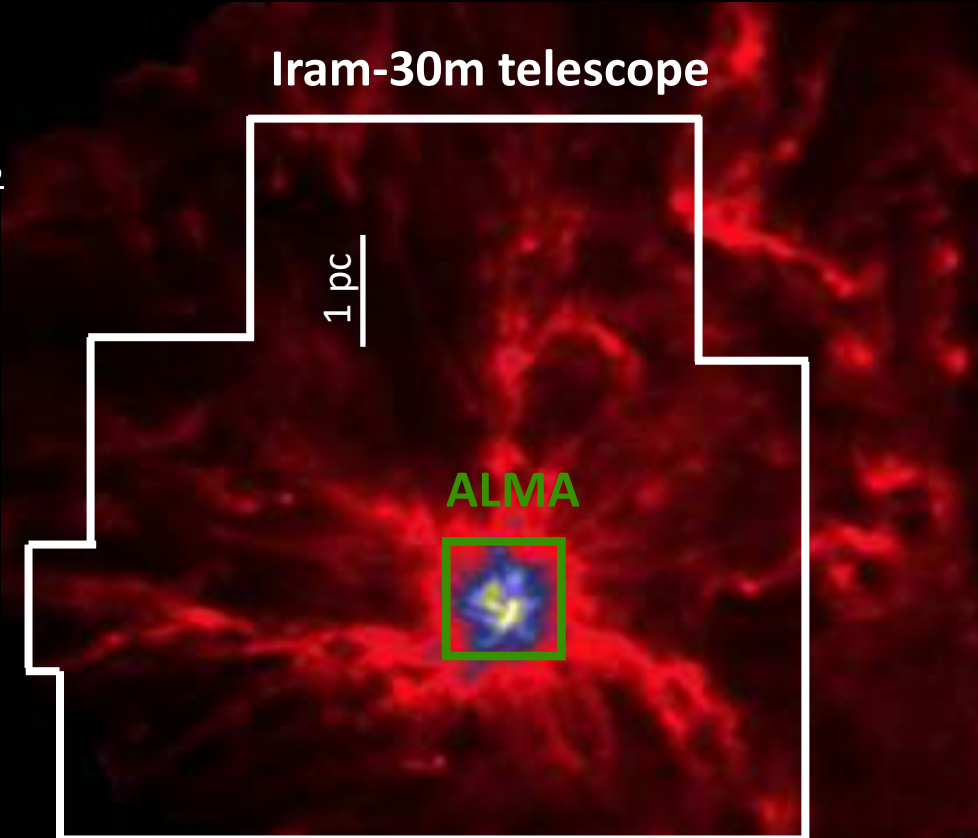
Pilleri + (2012); Treviño-Morales + (2014)

Study of the dynamical properties of Mon R2

Treviño-Morales + (2019)

Large scale observations

- **IRAM-30m telescope**
- (> 100 hours) at **3 mm band**
- ^{13}CO
- C^{18}O
- HNC
- N_2H^+



H_2 column density
From Herschel observations

Hub observations

- **ALMA**
- (7 hours) at **3 mm band**
- ^{13}CO
- C^{18}O
- CS
- $\text{H30}\alpha$
- SO

Treviño-Morales + (in prep.)

Dynamics of Cluster-forming hub-filament systems: The Mon R2 case

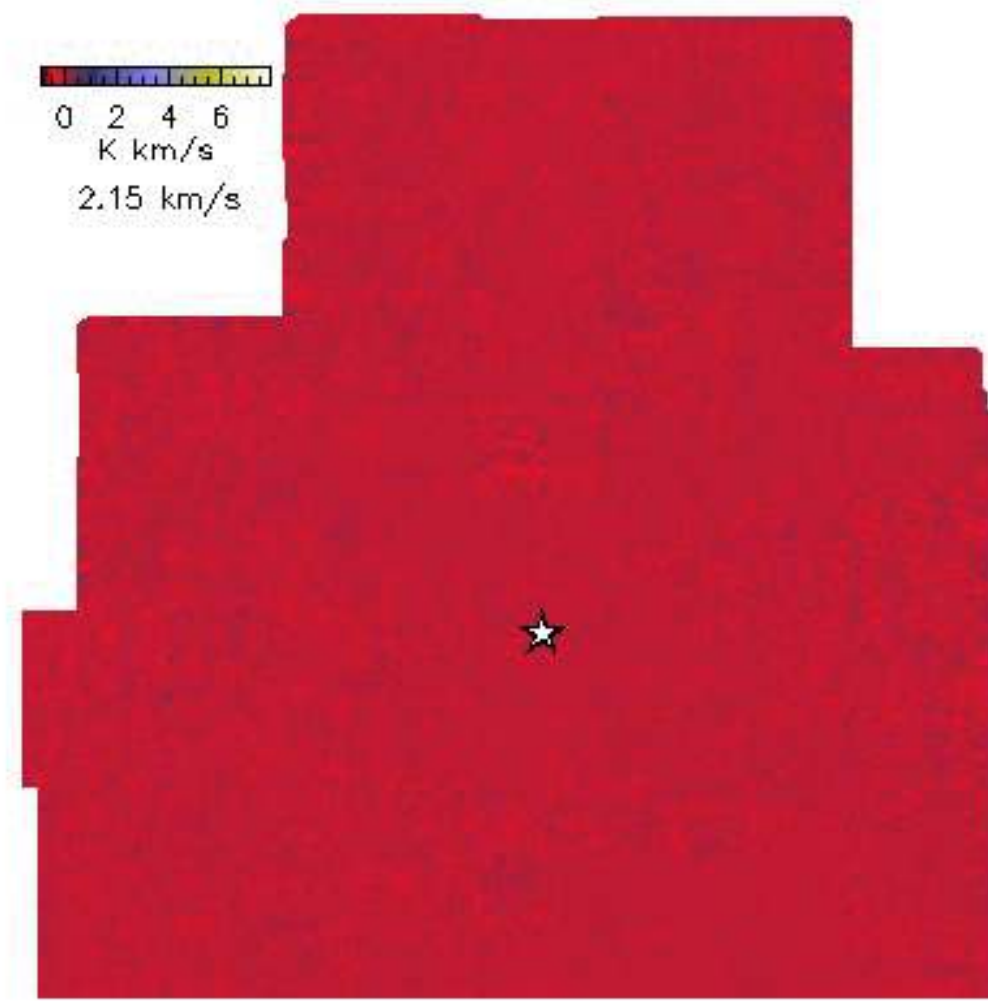
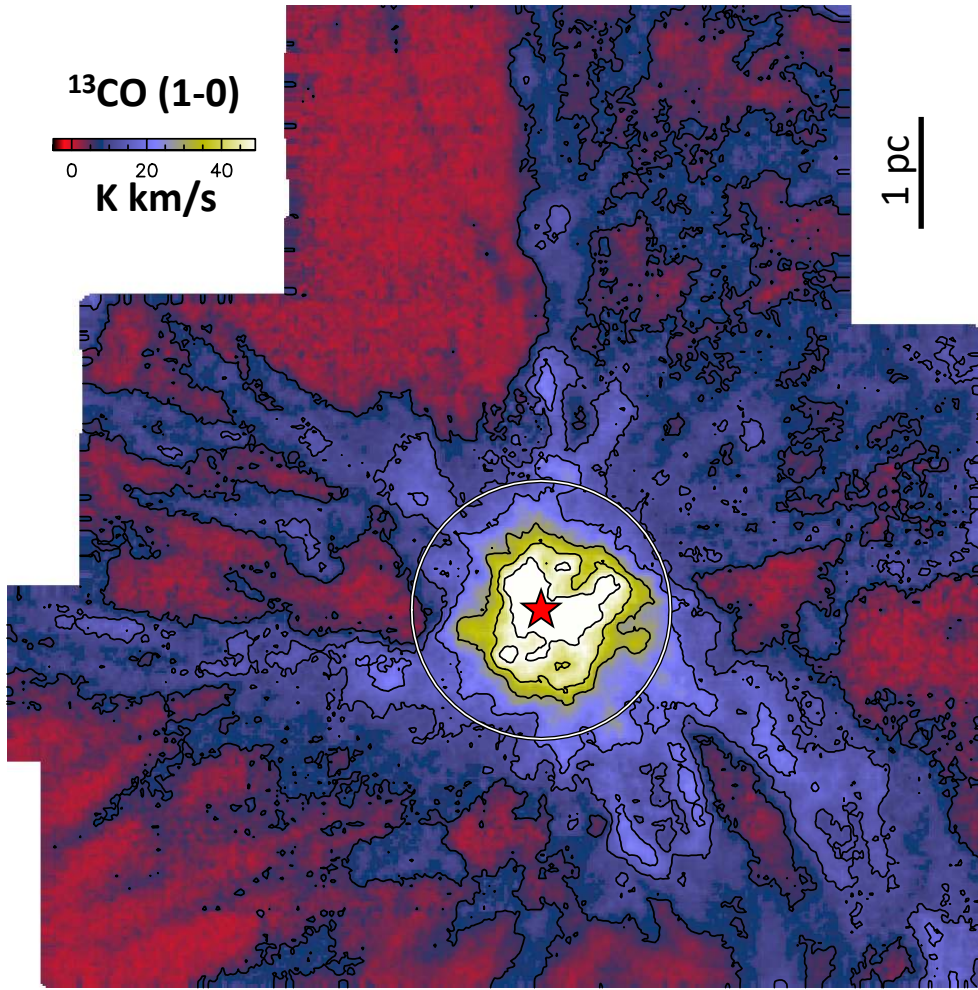
S. P. Treviño-Morales (Chalmers University), A. Fuente (Observatorio Astronómico Nacional), Á. Sánchez-Monge (Universität zu Köln), J. Kainulainen (Chalmers University), P. Didelon (Université Paris Diderot), S. Suri (Max-Planck Institute for Astronomy), N. Schneider (Universität zu Köln), J. Ballesteros-Paredes (Instituto de Radioastronomía y Astrofísica), Y. N. Lee (Institut de Physique du Globe de Paris), P. Hennebelle (Laboratoire AIM), P. Pilleri (Université de Toulouse), M. González-García (Instituto de Astrofísica de Andalucía), C. Kramer (Institut de Radioastronomie Millimétrique), S. García-Burillo (Observatorio Astronómico Nacional), A. Luna (Instituto Nacional de Astrofísica, Óptica y Electrónica), J. R. Goicoechea (Instituto de Física Fundamental, CSIC), P. Tremblin (Université Paris Diderot), and S. Geen (Universität zu Heidelberg)

Astronomy & Astrophysics 2019, arXiv e-prints, arXiv:1907.03524

Large-scale emission (30m observations)

Molecular emission is extended and **well correlated with the dust emission**

Treviño-Morales + (2019)

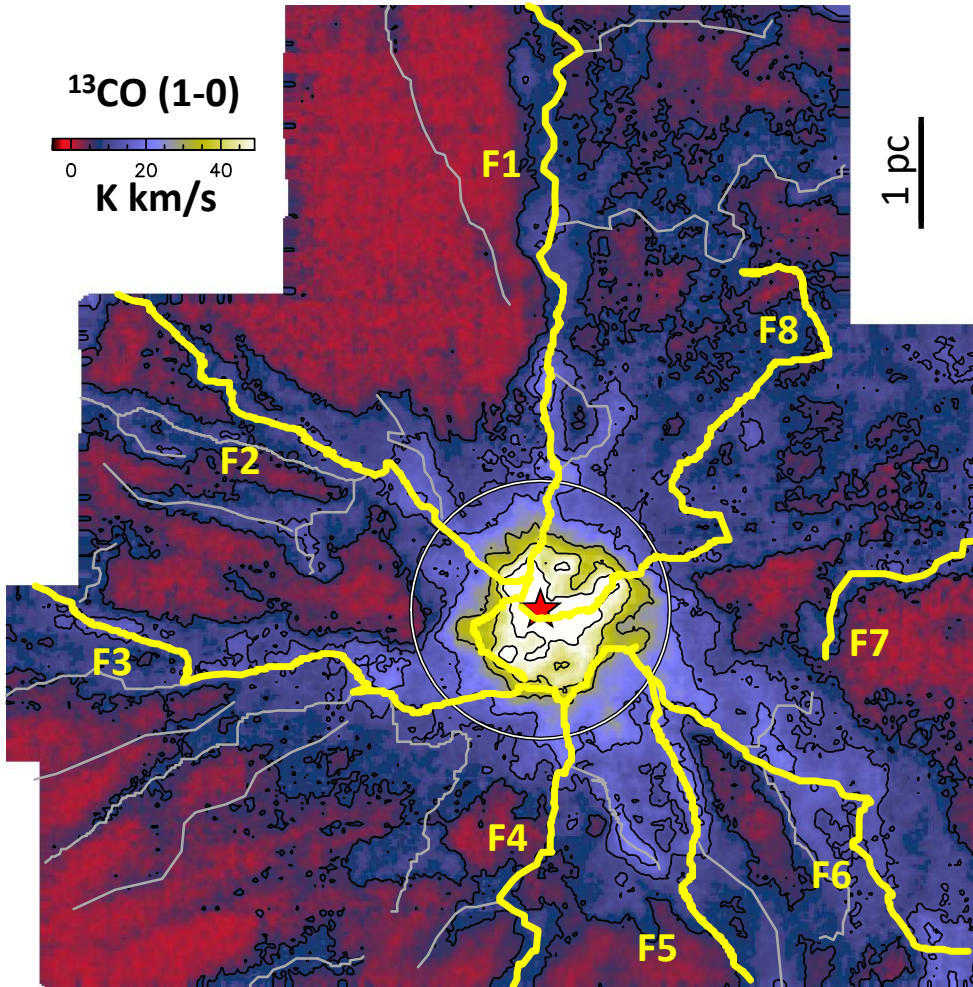


Channel maps from the ^{13}CO emission (intervals of 0.25 km/s)

Filaments: Stability (30m observations)

$M_{\text{total}} = 8300 M_{\odot}$; $M_{\text{hub}} = 2800 M_{\odot}$ (inner 250'');
 $M_{\text{fil}} = 2800 M_{\odot}$

Treviño-Morales + (2019)



$$M/L = 50 (M_{\odot} \text{ pc}^{-1})$$

$$(M/L)_{\text{crit}} = \frac{2\sigma_{\text{ther}}^2}{G} = 16.7 \left(\frac{T}{10\text{K}} \right) M_{\odot} \text{ pc}^{-1}$$

with $T \sim 15 \text{ K}$

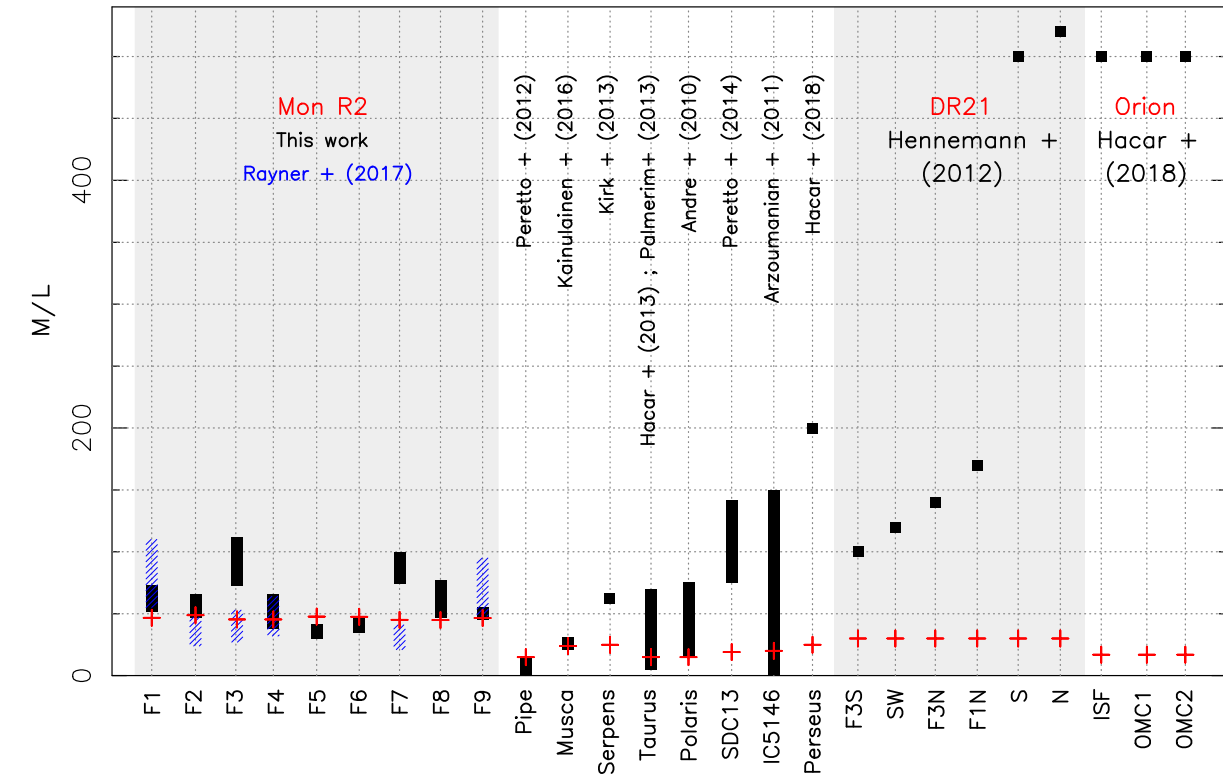
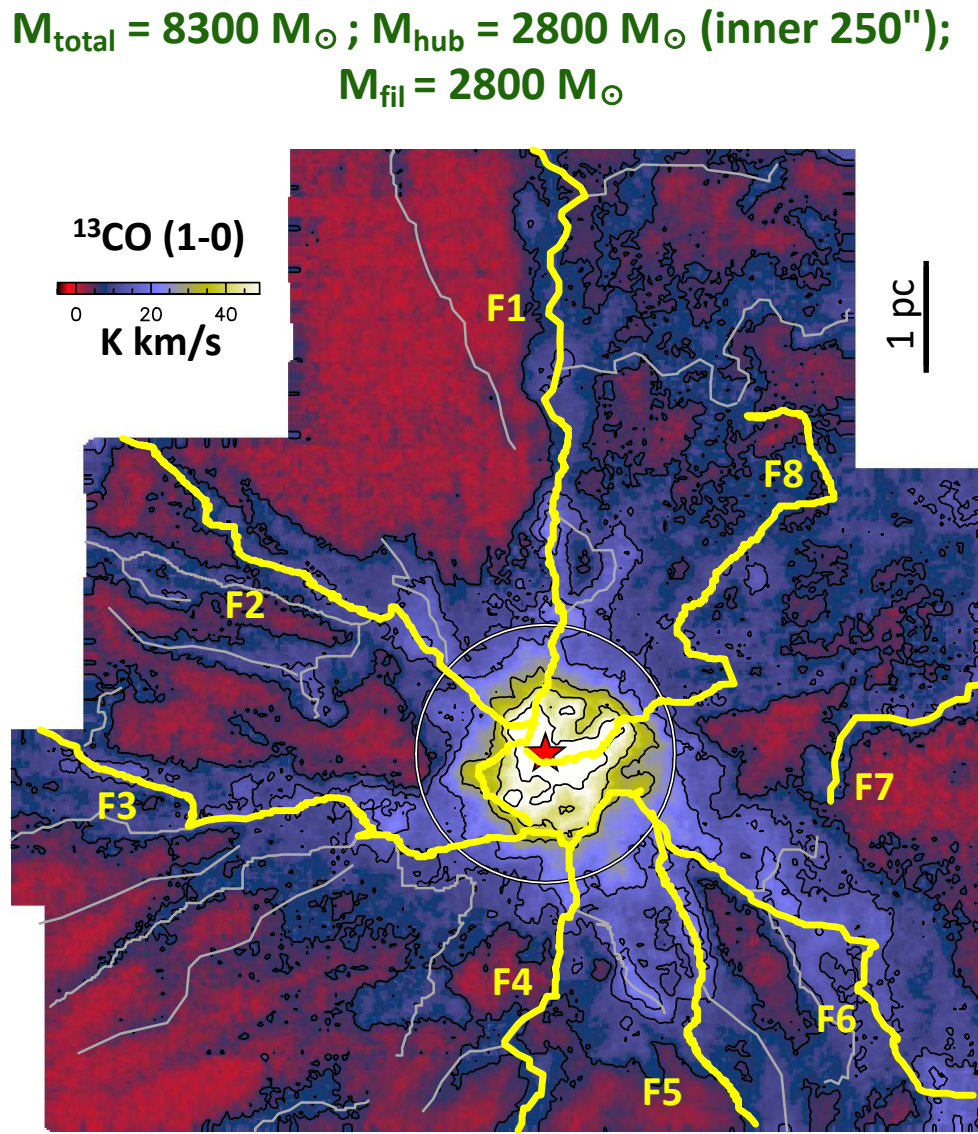
$$M/L_{\text{crit}} = 30 (M_{\odot} \text{ pc}^{-1})$$

Hints of fragmentation along the filaments

Ostriker (1964); Kirk + (2013); Nagasawa 1987;
Wang + 2014

Filaments: Stability (30m observations)

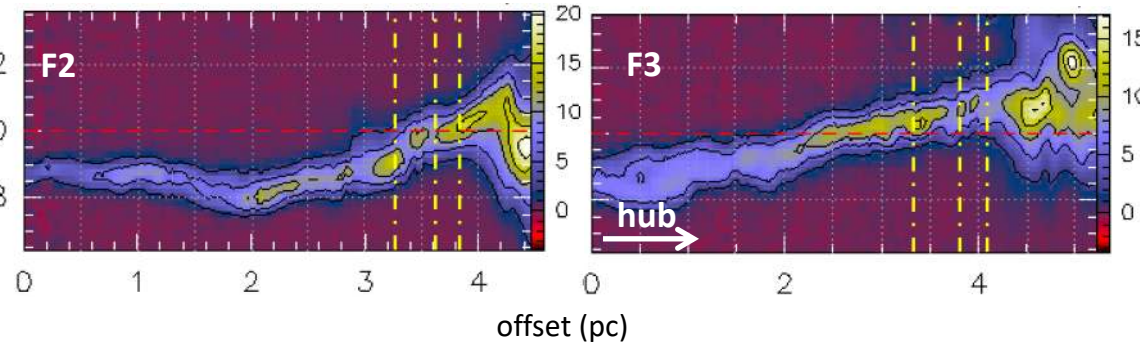
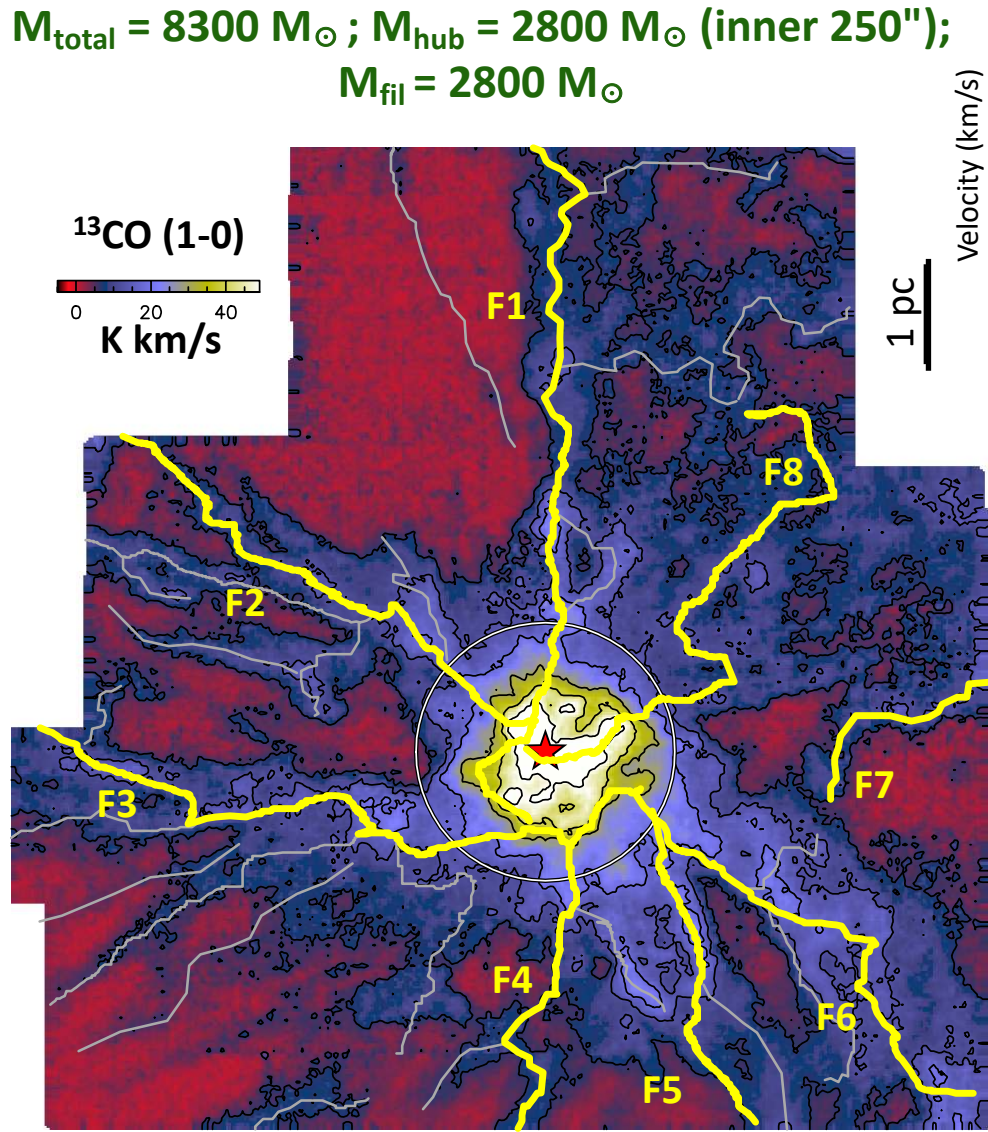
Treviño-Morales + (2019)



| | | |
|---------------|---|----------------------|
| Musca : | $M/L = 30 (M_{\odot} \text{ pc}^{-1})$ | Kainulainen + (2016) |
| Taurus (B211) | $M/L = 50 (M_{\odot} \text{ pc}^{-1})$ | Palmeirim + (2013) |
| DR21 | $M/L > 100 (M_{\odot} \text{ pc}^{-1})$ | Hennemann + (2012) |
| Orion A | $M/L = 500 (M_{\odot} \text{ pc}^{-1})$ | Hacar + (2018) |

Filaments: Dynamics (30m observations)

Treviño-Morales + (2019)



- **Velocity gradients** measured as the velocity difference between the extremes of the filament
- **Mass accretion rates**, assuming 45° of orientation

$$M_{\text{accr}} = \frac{\left(\frac{M}{L_{\text{obs}}} V_{\parallel \text{obs}}\right)}{\tan \alpha} = \frac{M \nabla V_{\parallel \text{obs}}}{\tan \alpha}$$

$$\begin{aligned} \Delta V &= 2 \text{ km/s} \\ M_{\text{acc}} &= 10^{-4} - 10^{-3} M_{\odot}/\text{yr} \end{aligned}$$

Timing a global collapse

For a hub-filament system presenting a global non-isotropic collapse, the gas flows through the filaments to form the central hub

$$\text{Mass-doubling time} = M(M_\odot)/M_{\text{acc}}(M_\odot \text{ yr}^{-1})$$

$$\text{Mass-doubling time} = 4-7.5 \text{ Myr}$$

$$M_{\text{hub}} \sim 3000 M_\odot$$

$$\text{Total mass accretion rate} = 4-7 \times 10^{-4} M_\odot \text{ yr}^{-1}$$

For $\sim 12 \times 10^{-4} M_\odot \text{ yr}^{-1}$ a slightly shorter is mass-doubling time ($\sim 2.5 \text{ Myr}$). Considering the gas density of $\sim 10^4 \text{ cm}^{-3}$ for Mon R2, the free-fall time is $\sim 3 \times 10^5 \text{ yr}$.

$$t_{\text{ff}} = (3\pi/(32G\rho))^{-(1/2)}$$

The mass-doubling time derived from the velocity gradients seen in the filaments is one order of magnitude larger than the free-fall time in Mon R2, suggesting a dynamically old region. If the initial density of the cloud is lower, and on the order of $\sim 5 \times 10^2 \text{ cm}^{-3}$, the free-fall time is in agreement with the mass-doubling time, suggesting a dynamically young region.

Global collapse!?

Smith et al. 2009; Gómez & Vázquez-Semadeni 2014; Vázquez-Semadeni et al. 2017; Ballesteros-Paredes et al. 2018; Lee & Hennebelle 2016, 2019

Lee & Hennebelle (2019) present simulations of a collapsing molecular cloud and summarize the main features of the process in (i) a global collapse forming a central stellar cluster, (ii) prominent filamentary structures, and (iii) stars forming along the radial filaments that feed the central cluster. The presence of radial filamentary structures like the one seen in MonR2 is more prominent in simulations with a low initial density. In this situation (case A of Lee & Hennebelle 2019) the global collapse precedes the formation of most of the stars. Contrary to that, for initially denser clouds (see case C of Lee & Hennebelle 2019), star formation activity is more widespread and the global collapse is less efficient, resulting in a web-like cloud instead of a radially filamentary cloud. A different interpretation for the generation of a radial filamentary structures in a molecular cloud, is presented in Ballesteros-Paredes et al. (2015), where the turbulent crossing time is \sim 6-7 times longer than the sound crossing time (consistent with the obtained in the case A of Lee & Hennebelle 2019).

*Global collapsing cloud where the filaments feed
the central hub*

Fragmentation

*An expanding HII region braking out the
filaments*

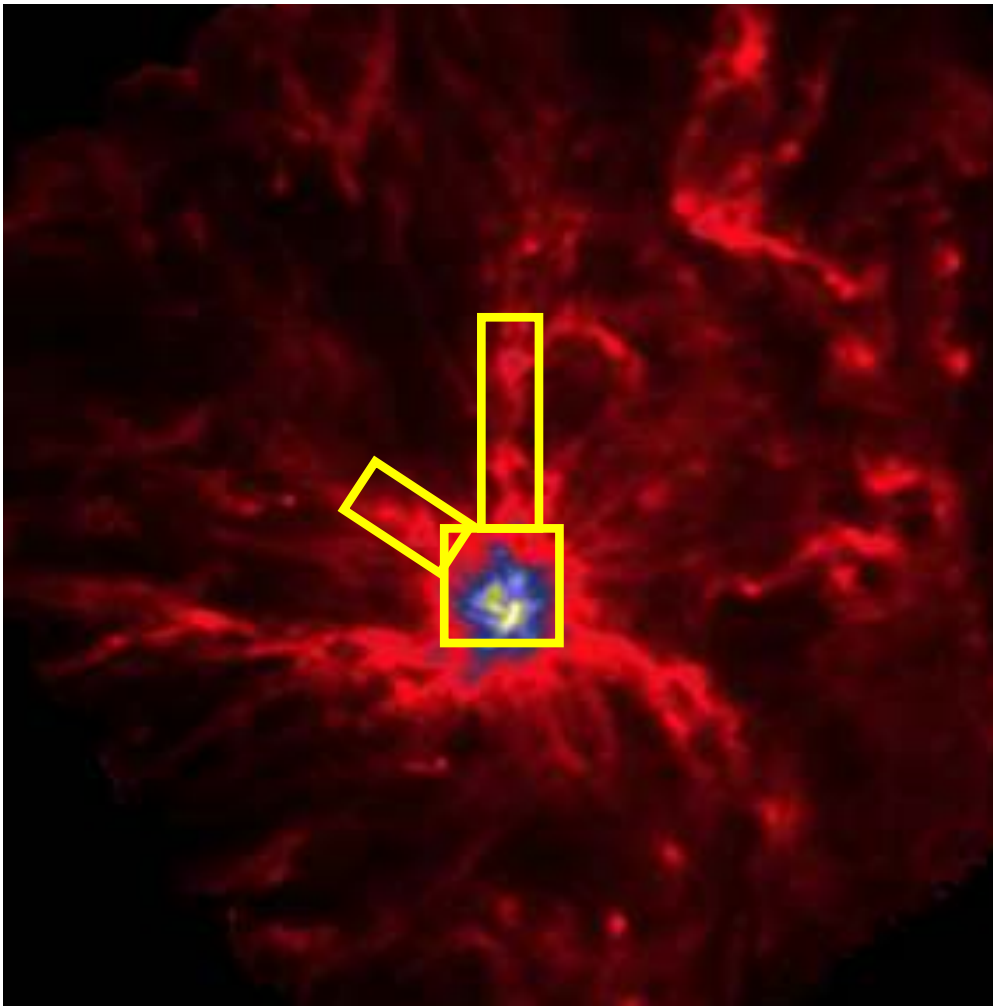
Dynamical signs of a rotating accreting spiral structure

S. P. Treviño-Morales (Chalmers University), Á. Sánchez-Monge (Universität zu Köln), J. Kainulainen (Chalmers University), A. Fuente (Observatorio Astronómico Nacional), S. Suri (Max-Planck Institute for Astronomy), P. Rivière-Marichalar (Observatorio Astronómico Nacional), J. Orkisz (Chalmers University), P. Didelon (Université Paris Diderot), N. Schneider (Universität zu Köln), J. Ballesteros-Paredes (Instituto de Radioastronomía y Astrofísica), Y. N. Lee (Institut de Physique du Globe de Paris), P. Hennebelle (Laboratoire AIM), M. González-García (Instituto de Astrofísica de Andalucía), P. Tremblin (Université Paris Diderot)

Astronomy & Astrophysics 2019, in preparation.

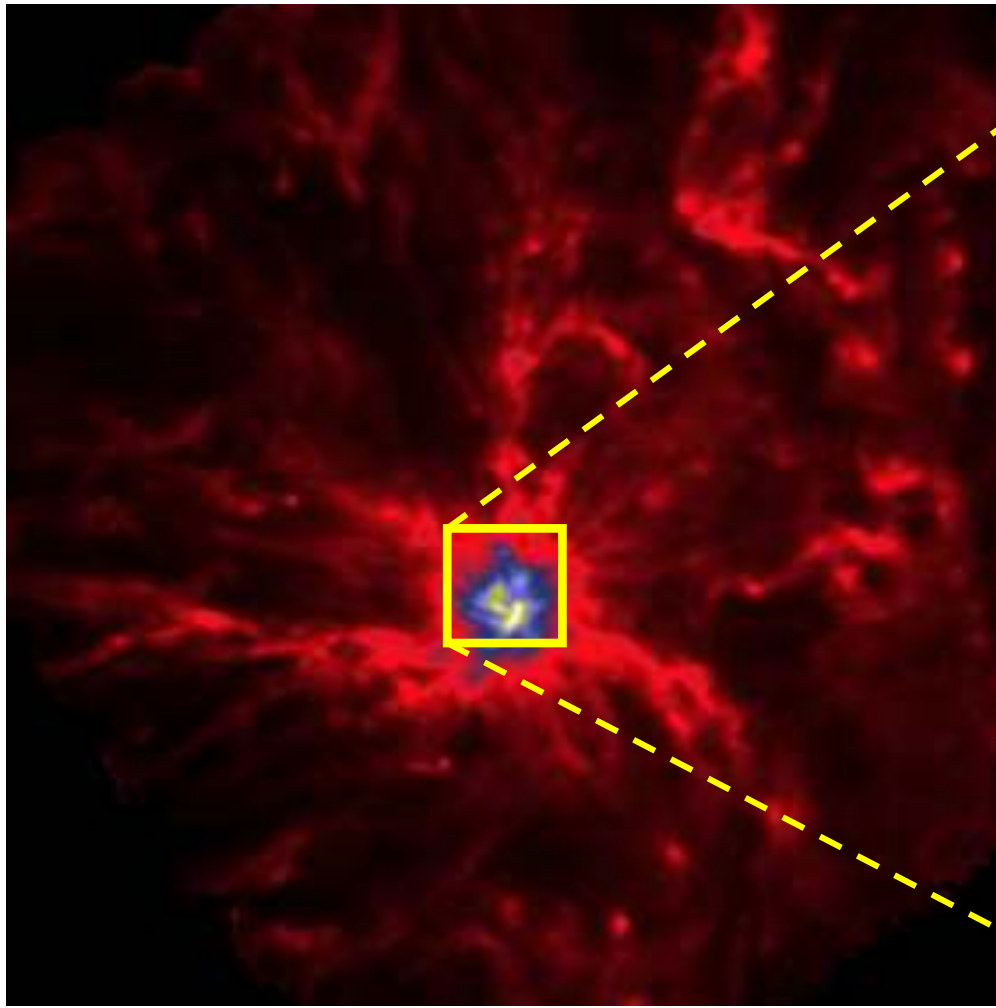
Dynamical signs of a rotating accreting spiral structure

Didelon + (2015)

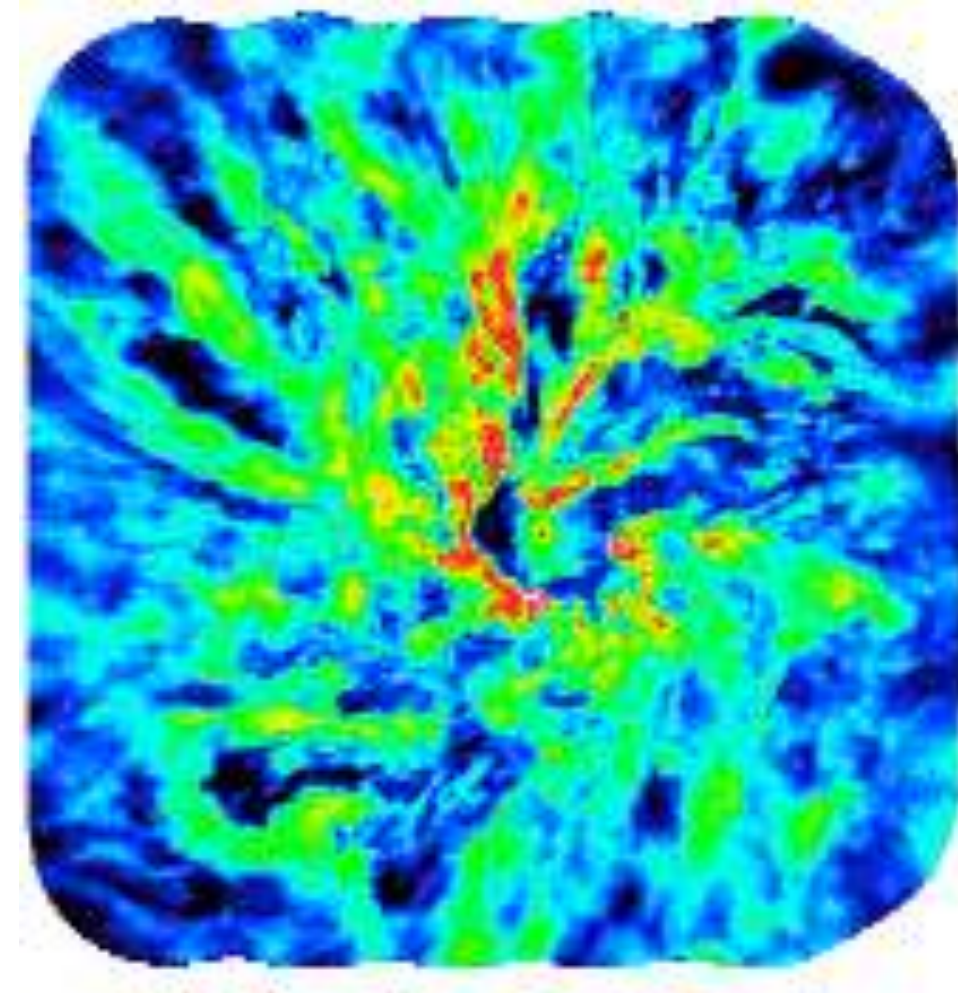


Dynamical signs of a rotating accreting spiral structure

Didebon + (2015)



H_2 column density

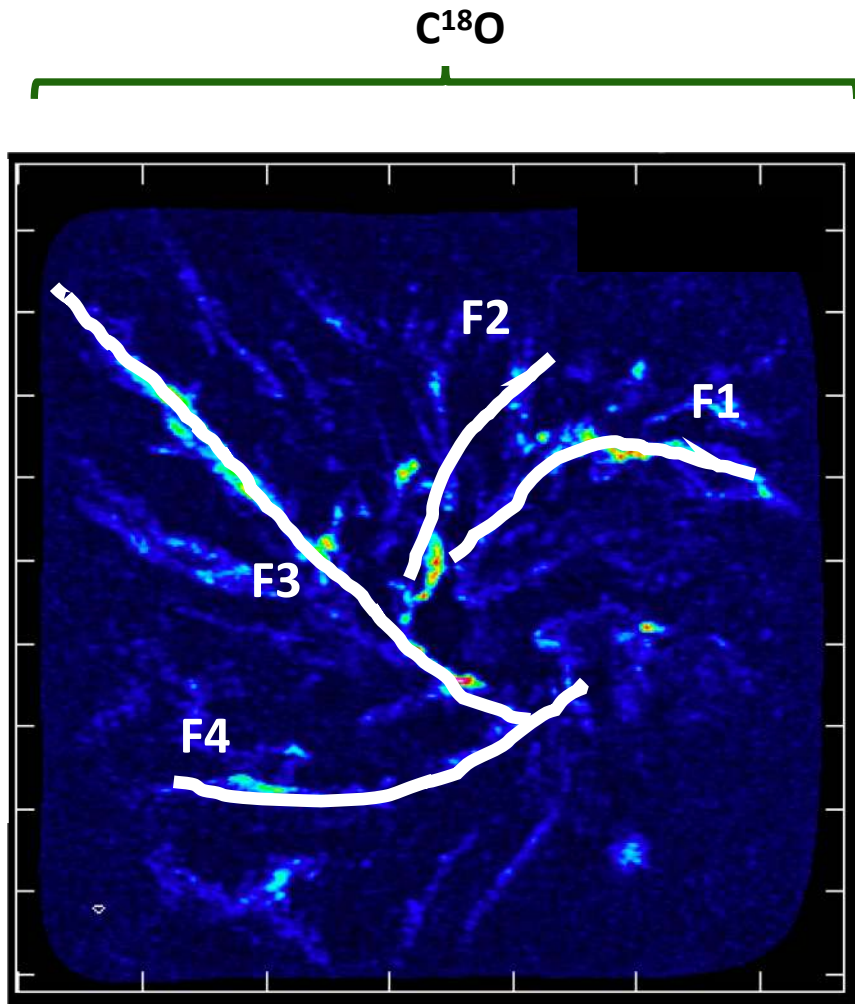


^{13}CO (1-0)

Treviño-Morales + (in prep.)

Dynamical signs of a rotating accreting spiral structure

Treviño-Morales + (in prep.)



Filaments in the
central Hub

- $\Delta V \sim 0.5\text{--}2 \text{ km s}^{-1}/\text{pc}$
- $M = 100\text{--}400 M_{\odot}$
- $M_{\text{acc}} = 0.5\text{--}4 \times 10^{-4}$

Filament Identification
Keplerian rotation??
3D structure??

Filaments inside the hub are transonic

Are spiral filamentary structures affecting the star-forming?

MUSCLE W49: A MULTI-SCALE CONTINUUM AND LINE EXPLORATION OF THE MOST LUMINOUS STAR FORMATION REGION IN THE MILKY WAY. I. DATA AND THE MASS STRUCTURE OF THE GIANT MOLECULAR CLOUD

R. GALVÁN-MADRID¹, H. B. LIU², Z.-Y. ZHANG^{3,4}, J. E. PINEDA^{1,5,6}, T.-C. PENG¹, Q. ZHANG⁷, E. R. KETO⁷, P. T. P. HO^{2,7}, L. F. RODRÍGUEZ^{8,9}, L. ZAPATA⁸, T. PETERS¹⁰, AND C. G. DE PREE¹¹

ALMA RESOLVES THE SPIRALING ACCRETION FLOW IN THE LUMINOUS OB CLUSTER-FORMING REGION G33.92+0.11 [Download](#)

HAUYU BAOBAB LIU¹, ROBERTO GALVÁN-MADRID², IZASKUN JIMÉNEZ-SERRA³, CARLOS ROMÁN-ZÚÑIGA⁴, QIZHOU ZHANG⁵, ZHIYUN LI⁶, AND HUEI-R



CLOUD STRUCTURE OF GALACTIC OB CLUSTER-FORMING REGIONS FROM COMBINING GROUND- AND SPACE-BASED BOLOMETRIC OBSERVATIONS

YUXIN LIN¹, HAUYu BAOBAB LIU², DI LI^{1,3}, ZHI-YU ZHANG^{4,2}, ADAM GINSBURG², JAIME E. PINEDA⁵, LEI QIAN¹, ROBERTO GALVÁN-MADRID⁶, ANNA FAYE MCLEOD², ERIK ROSOLOWSKY⁷, JAMES E. DALE^{8,9}, KATHARINA IMMER², ERIC KOCH⁷

Revealing a spiral-shaped molecular cloud in our galaxy – Cloud fragmentation under rotation and gravity

Guang-Xing Li^{1,2}, Friedrich Wyrowski², and Karl Menten²

The physical and chemical structure of Sagittarius B2

II. Continuum millimeter emission of Sgr B2(M) and Sgr B2(N) with ALMA

Á. Sánchez-Monge¹, P. Schilke¹, A. Schmiedeke^{1,2}, A. Ginsburg^{3,4}, R. Cesaroni⁵, D.C. Lis^{6,7}, S.-L. Qin⁸, H.S.P. Müller¹, E. Bergin⁹, C. Comito¹, and Th. Möller¹

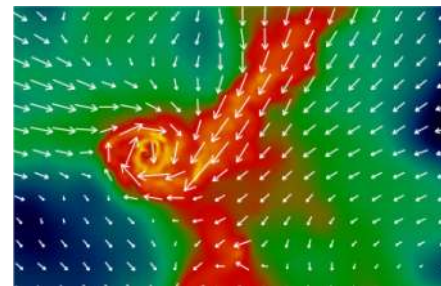
A KEPLERIAN-LIKE DISK AROUND THE FORMING O-TYPE STAR AFGL 4176

KATHARINE G. JOHNSTON¹, THOMAS P. ROBITAILLE², HENRIK BEUTHER², HENDRIK LINZ², PAUL BOLEY³, ROLF KUIPER^{4,2}, ERIC KETO⁵, MELVIN G. HOARE¹ AND ROY VAN BOEKEL²
(Accepted October 8, 2018)

FILAMENTS IN SIMULATIONS OF MOLECULAR CLOUD FORMATION

GILBERTO C. GÓMEZ AND ENRIQUE VÁZQUEZ-SEMADENI

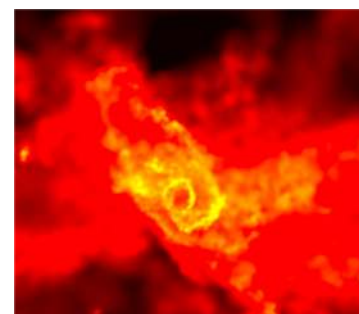
Centro de Radioastronomía y Astrofísica, Universidad Nacional Autónoma de México, Campus Morelia Apartado Postal 3-72, 58090 Morelia, Michoacán, Mexico
Received 2013 August 26; accepted 2014 July 17; published 2014 August 6



Rotation in young massive star clusters

Michela Mapelli^{1*}

¹INAF-Osservatorio Astronomico di Padova, Vicolo dell'Osservatorio 5, I-35122, Padova, Italy michela.mapelli@oapd.inaf.it



Spiral features converging in the central cluster

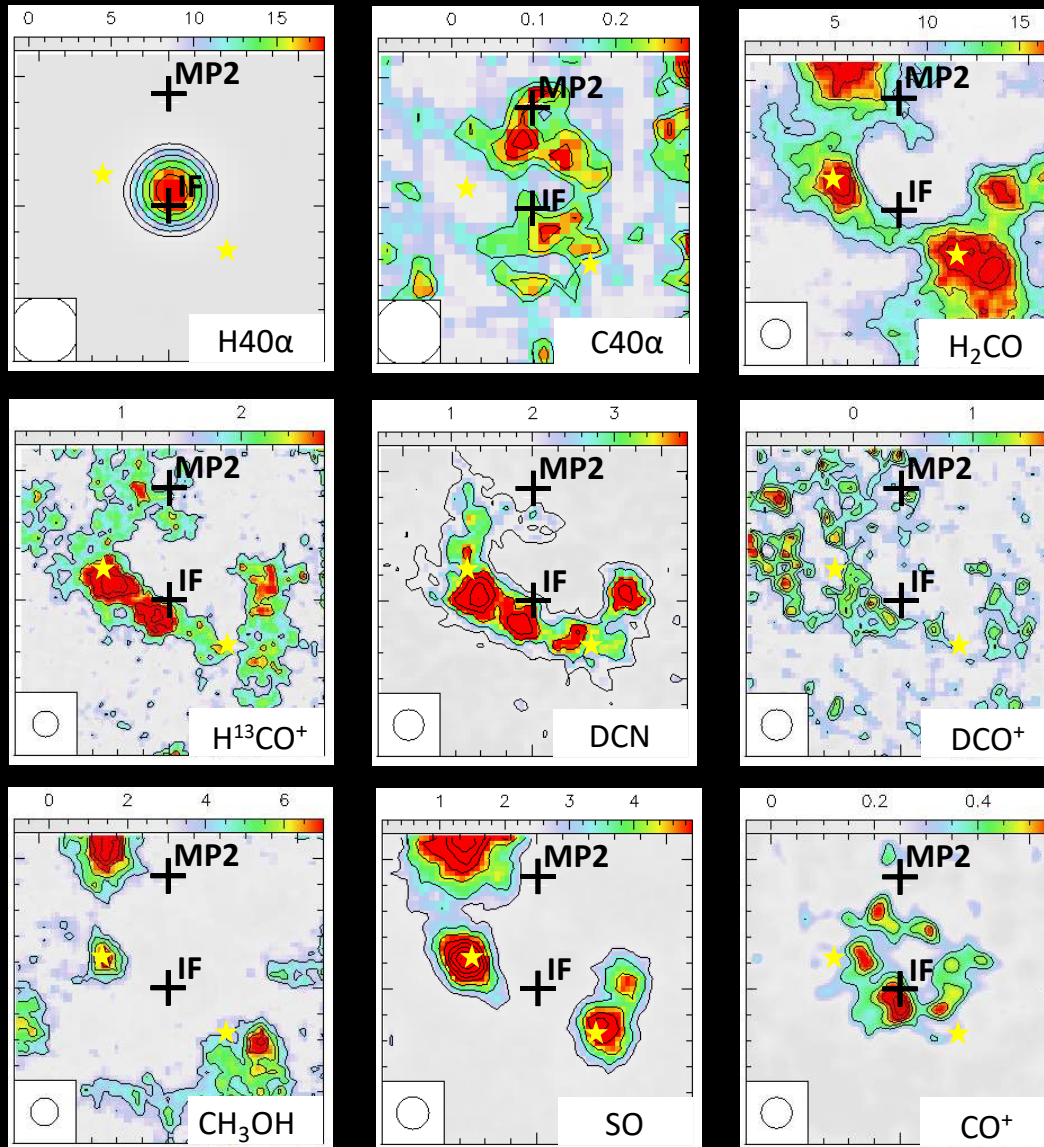
Sub-structures reminiscent to fibers

Similar structures seen in other OB clusters and simulations

A brief view to the chemical complexity

- Radio Recombination Lines
- Deuterated molecules
- Sulphurated molecules
- Complex molecules
- Hydrocarbons
- Nitrogenated species
- Ionic species

≈ 60 different species grouped in *families*



Treviño-Morales et al (2014;2016)

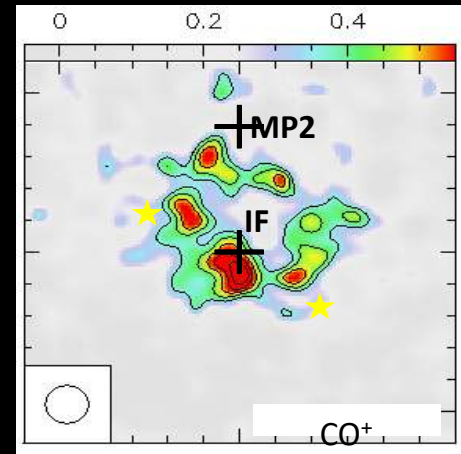
A brief view to the chemical complexity

Reactive ions are destroyed in almost every collision with H and H₂ and recombine rapidly with e⁻.

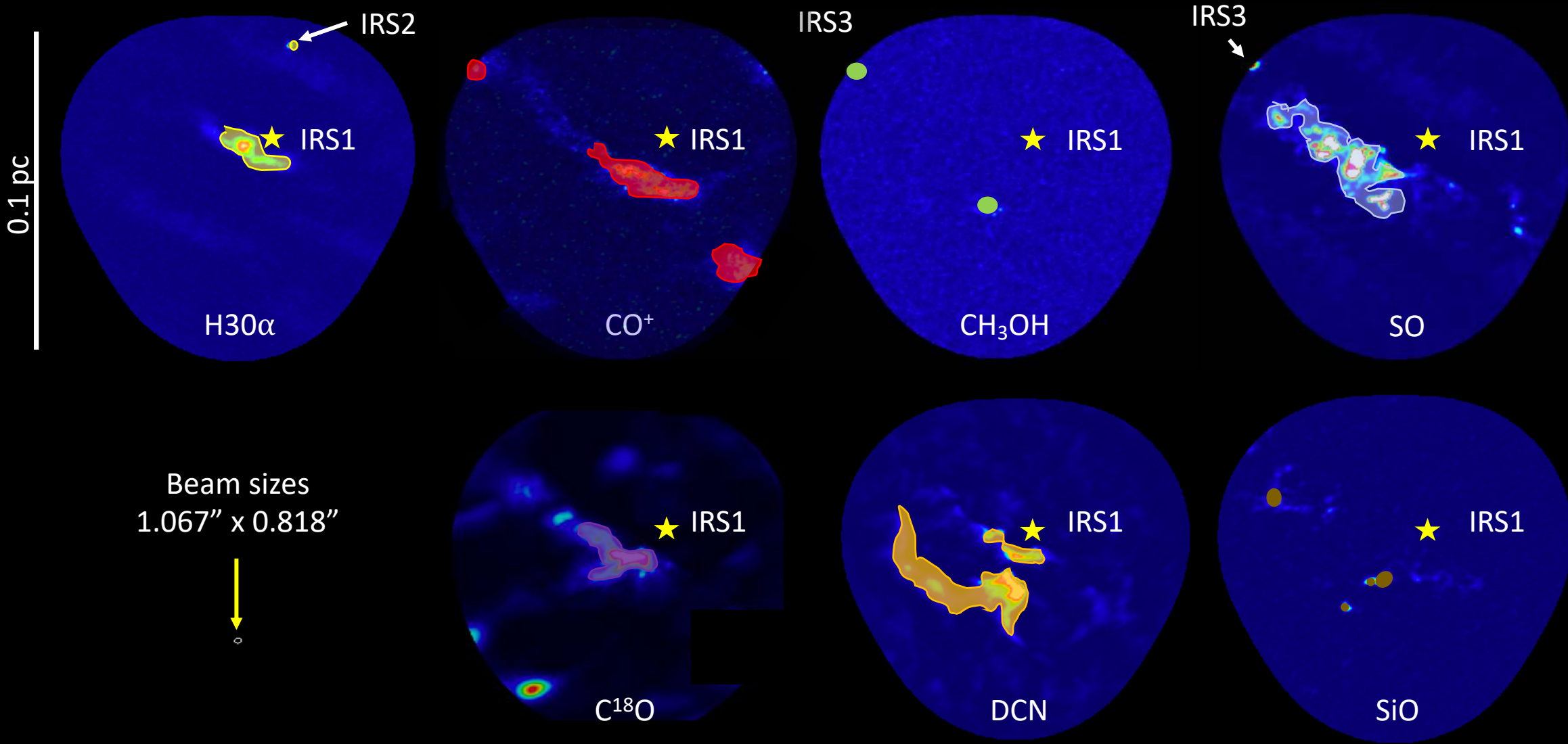
High CO⁺ abundance at the HI/H₂ interface ($A_V \approx 1$ mag) of dense PDRs
(Sternberg & Dalgarno 1995)

Produced by the C⁺ + OH → CO⁺ + H reaction.

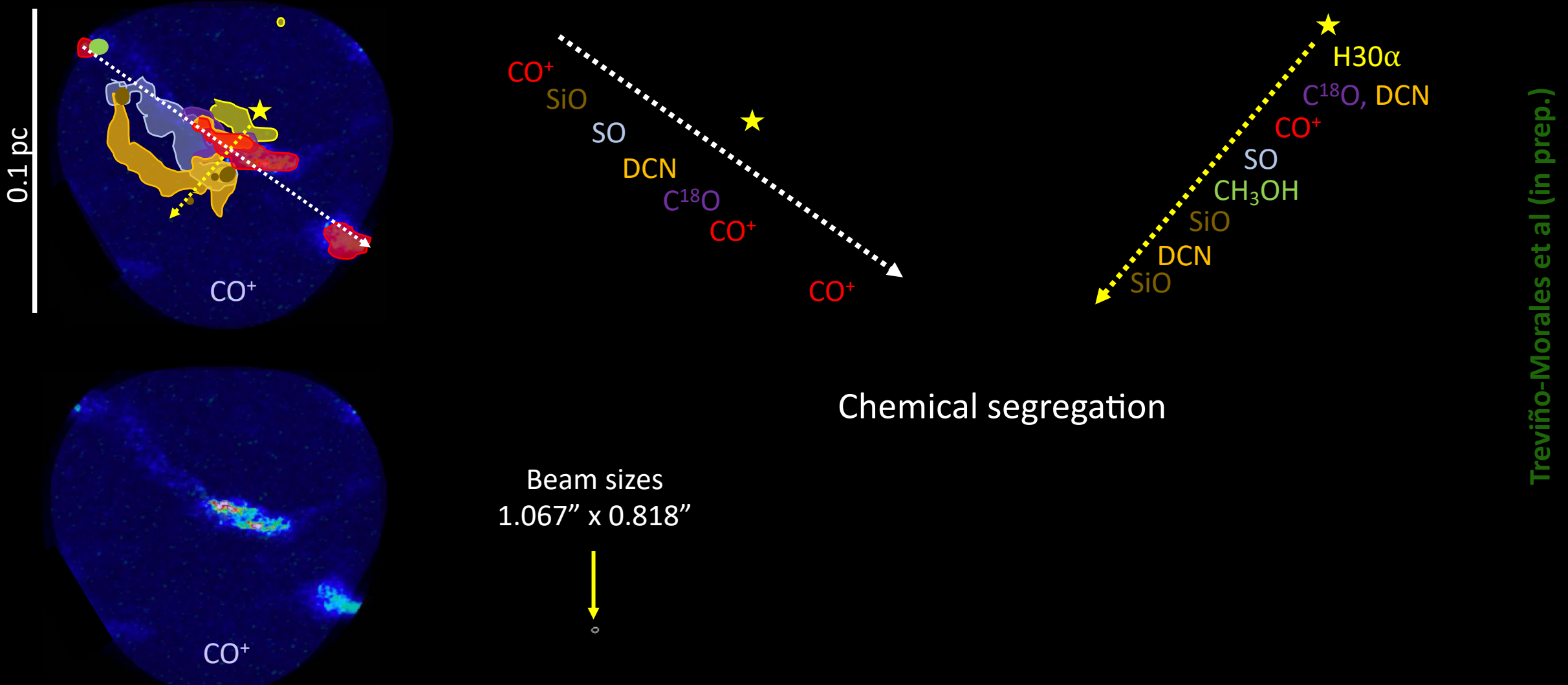
Has been detected in several PDRs, such as the M17SW, Orion Bar, NGC 7027, NGC 7023 (Latter et al. 1993; Stoerzer et al. 1995; Fuente & Martín-Pintado 1997; Fuente et al. 2003), G29.96, MonR2 (Rizzo et al. 2003) and S140 (Savage & Ziurys 2004).



A brief view to the chemical complexity



A brief view to the chemical complexity



Chemical segregation into the hub

Dense warm clumps

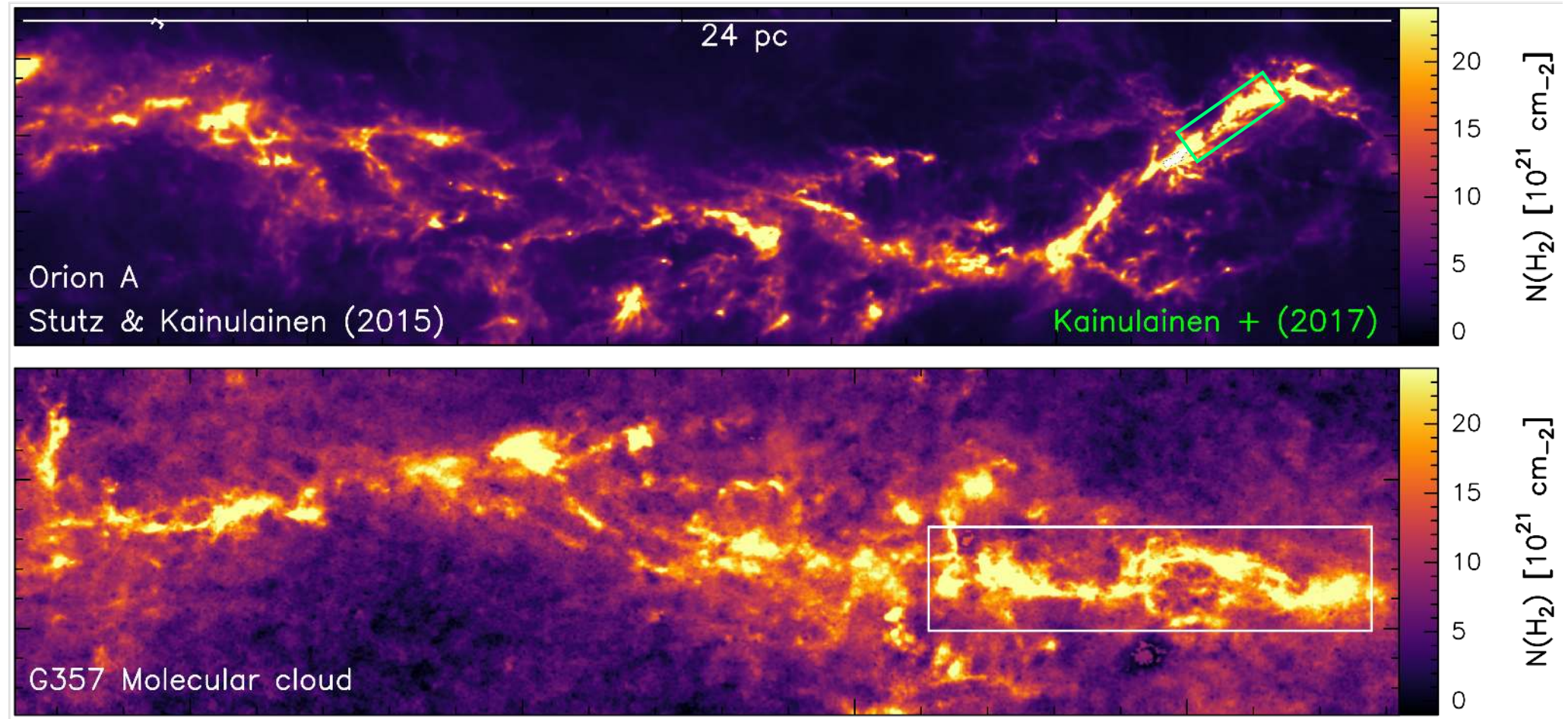
Hints of photoevaporation

Evolutionary sequence for the fragmentation of high line-mass filaments

S. P. Treviño-Morales (Chalmers University), J. Kainulainen (Chalmers University), M. Zhang (), J. Orkisz (Chalmers University), H. Beuter (), S. Clarke (), A. Stutz ()

Astronomy & Astrophysics, in preparation.

Evolutionary sequence for the fragmentation of high line-mass filaments



Aim: Develop an evolutionary sequence for **high line-mass filaments** by characterizing fragmentation of an *early-stage* filament and compare that with the evolved ISF.

Evolutionary sequence for the fragmentation of high line-mass filaments

Integral shaped filament (ISF)

- Located at ~ 420 pc
- Line-mass of $400 M_{\odot}/pc$
- High-mass star formation
- About 8 pc of longitude

G357

- Located at ~ 3 Kpc ($I = 357.7$, $b = -0.38$)
- Line-mass of $\sim 300 M_{\odot} /pc$
- harbors very few protostars
(deficiency of sub-mm sources, 24 μm sources, and red near-infrared sources.)
- Expected to form stars in the future
- Densest filament with about 8 pc of longitude

The G357 cloud morphology and mass are very similar to Orion A

Evolutionary sequence for the fragmentation of high line-mass filaments

Integral shaped filament (ISF)

12marray

- Primary beam $\sim 60''$
- Max recoverable scale $25''$
- Synthesized beam $3.2'' \times 1.7''$
- Achieved rms of 0.14 mJy/beam

ACA

- Primary beam $\sim 105''$
- Max recoverable scale $42''$
- Synthesized beam $19.9'' \times 10''.3$
- Achieved rms 2.3 mJy/beam

G357

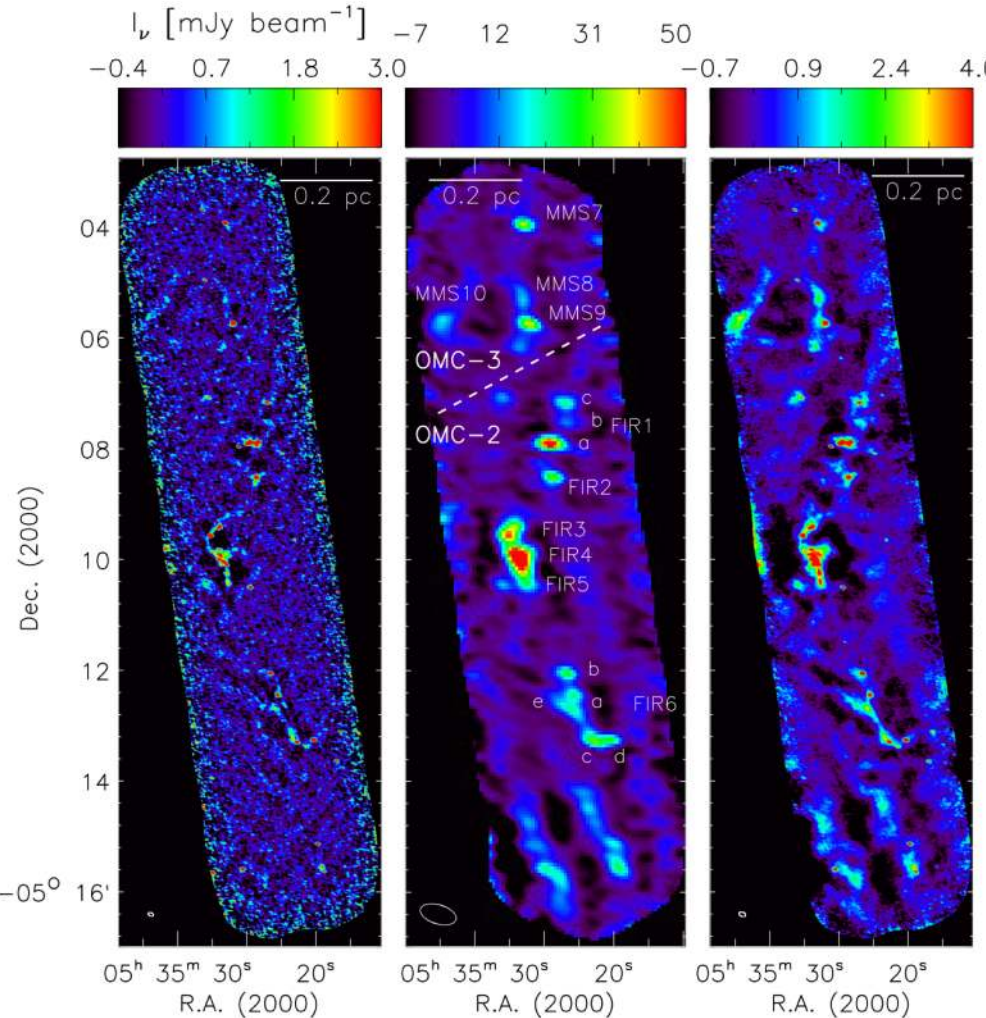
12m array

- Primary beam $\sim 63''$
- Max recoverable scale $32''$
- Synthesized beam $0.34'' \times 0.32''$
- Achieved rms of 0.2 mJy/beam

ACA

- Primary beam $\sim 107''$
- Max recoverable scale $55''$
- Synthesized beam $18'' \times 9''$
- Achieved rms 2.0 mJy/beam

Evolutionary sequence for the fragmentation of high line-mass filaments



- **43 cores** (26 corresponds with protostars)
- **Fluxes between 5 and 40 mJy**
- Starless cores show strong grouping
- **Groups correspond** to the gas morphology traced by the *Herschel column density map*
- Density profile along the filament show that the predictions for **Jeans' fragmentation scale is** $\sim 10000\text{AU}$ and for the filamentary **gravitational fragmentation scale is** $\sim 40000\text{AU}$.
- **Gravitational fragmentation is an important process**, even though our understanding of how exactly it proceeds is incomplete.

(Kainulainen + 2017)

Evolutionary sequence for the fragmentation of high line-mass filaments

- Located at ~ 3 Kpc ($l = 357.7$, $b = -0.38$)
- Dense cloud with line-mass of $\sim 300 M_{\odot} / pc$
- The cloud morphology and mass is very similar to Orion A
- Deficiency of sub-mm and red near-infrared sources
- Expected to form stars in the future

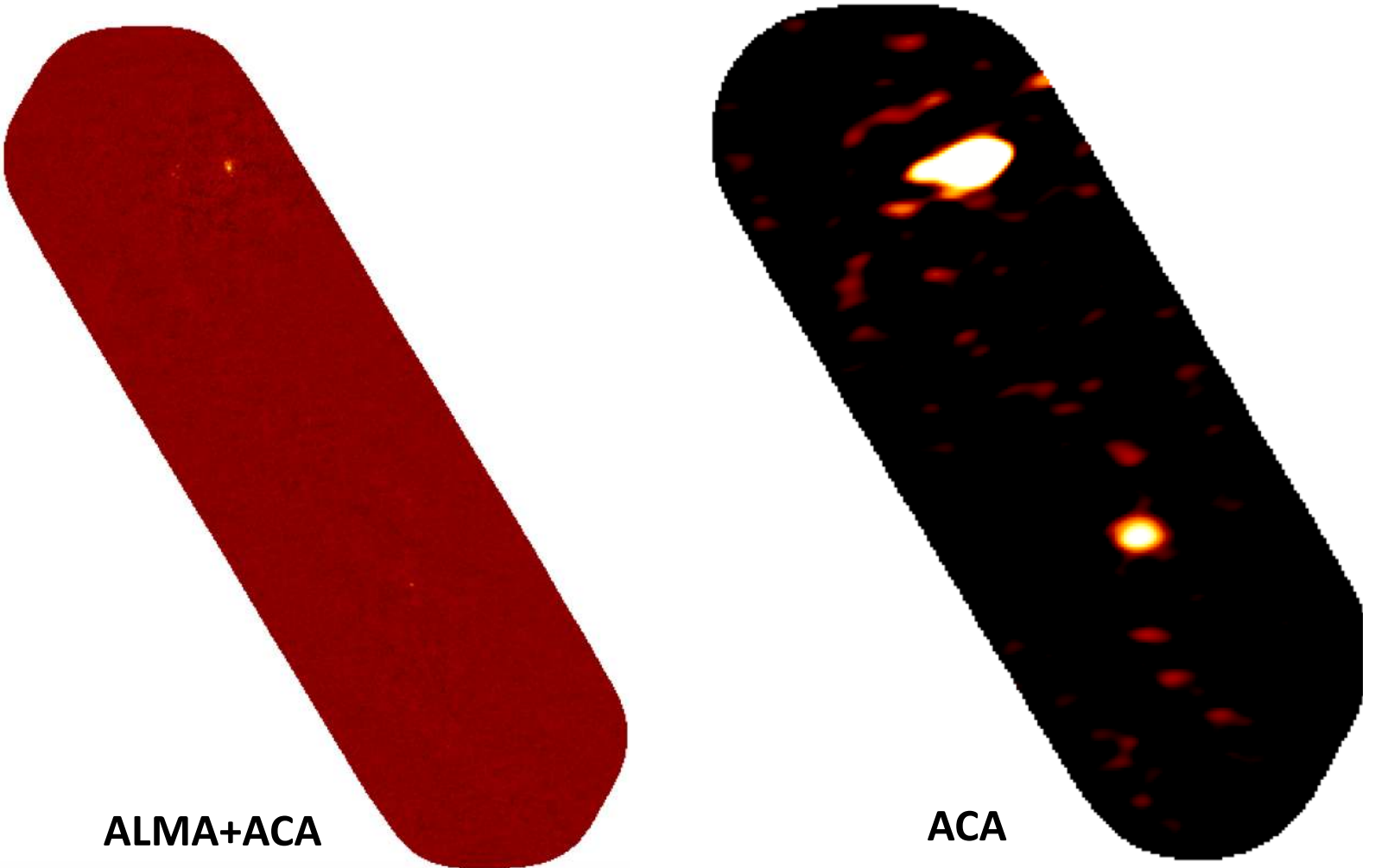
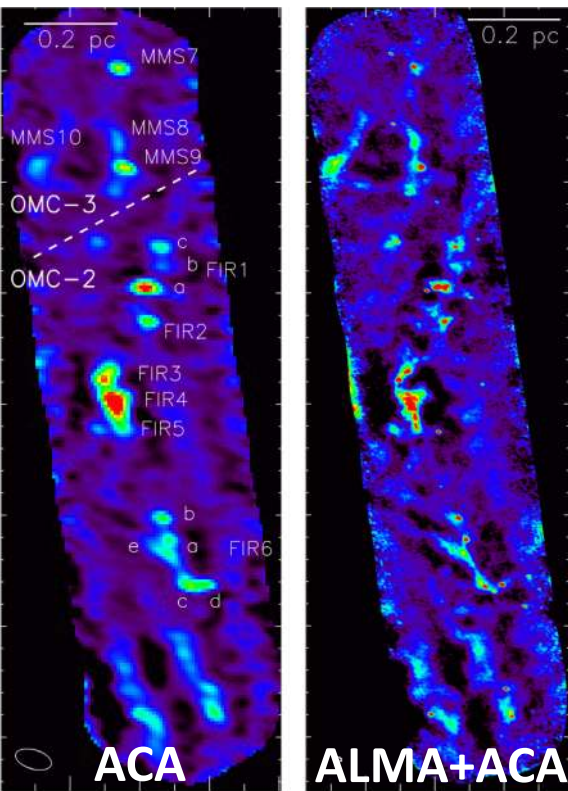
Coverage of ALMA Study
3 mm continuum and N₂H⁺
emission

7 pc

Treviño-Morales, Kainulainen,
Orkisz, Zang, Beuther, Stutz

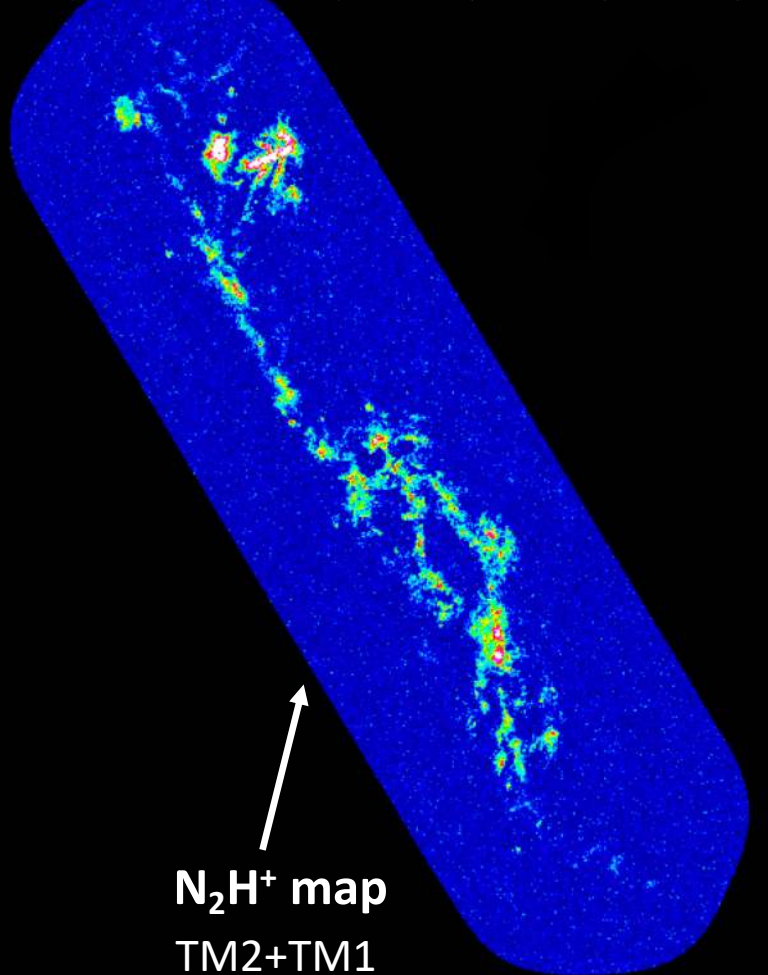
Evolutionary sequence for the fragmentation of high line-mass filaments

ISF



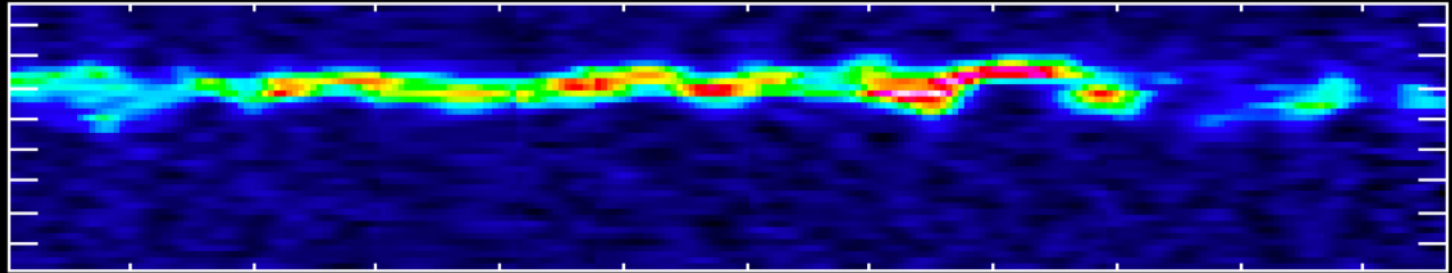
The G357 has a “lack” of continuum extended emission

Evolutionary sequence for the fragmentation of high line-mass filaments

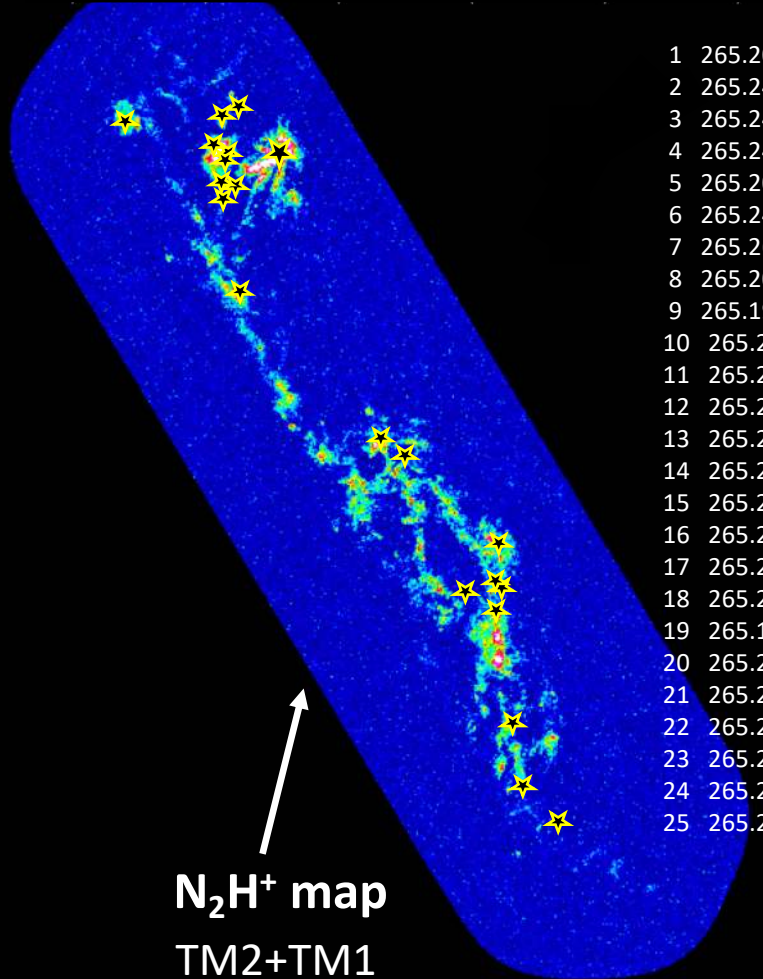


Identification of compact objects

- GaussClumps (CUPID)
- 25 objects
- Resolved D of a few 1000 AU
- M=0.3-3.5 M_⊙



Evolutionary sequence for the fragmentation of high line-mass filaments



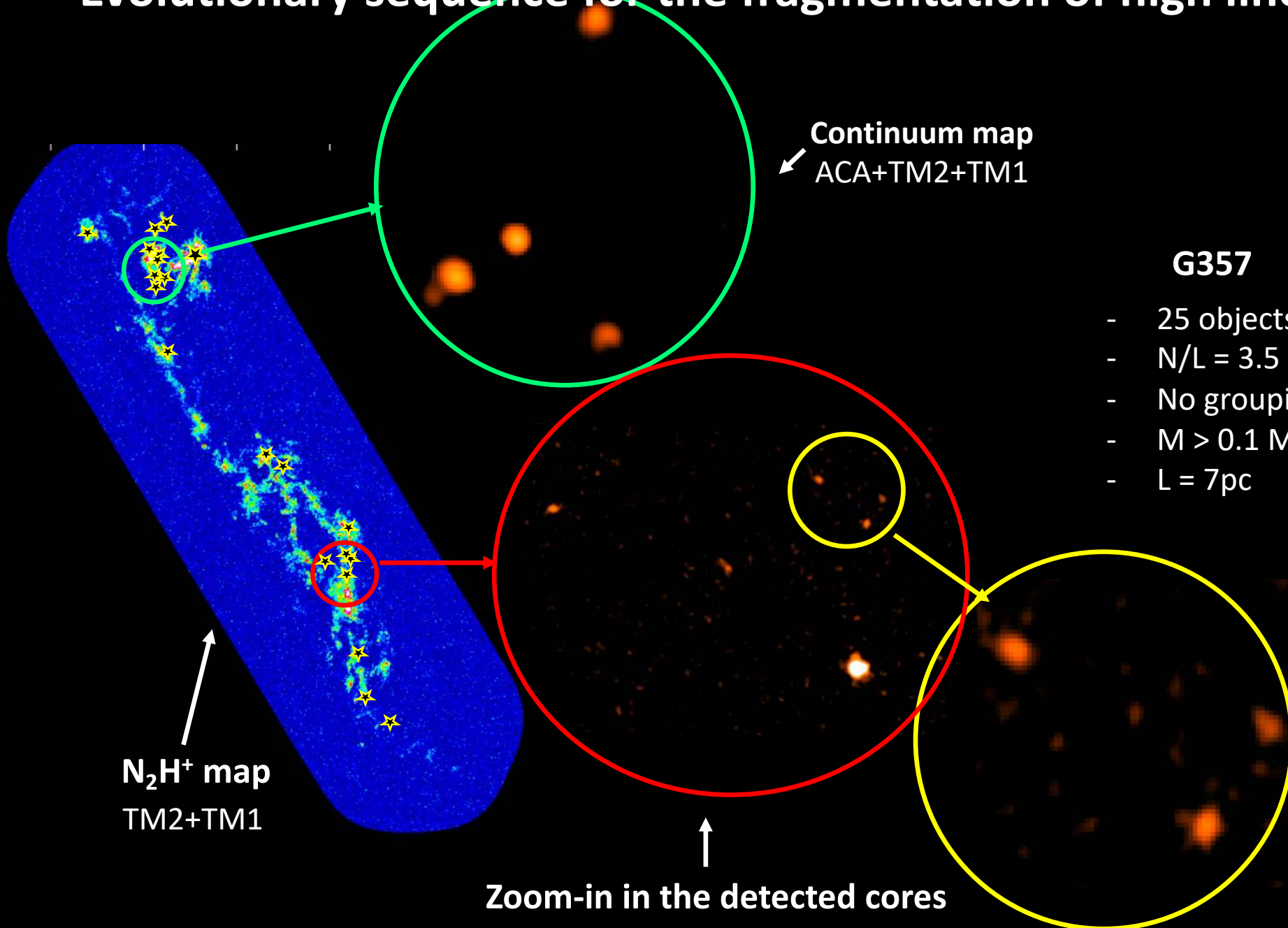
N_2H^+ map

TM2+TM1

| no | ra | dec | x | y | fwhm_x | fwhm_y | size_x | size_y | p_flux | totalflux | pa | edge | stdev | snr |
|----|------------|------------|----------|----------|--------|--------|--------|--------|----------|-----------|---------|-------|-----------|---------|
| 1 | 265.204681 | -31.248840 | 4395.050 | 2938.180 | 8.690 | 7.530 | 0.250 | 0.220 | 0.002714 | 0.202603 | -9.940 | 0.000 | 2.420E-05 | 112.136 |
| 2 | 265.248230 | -31.184158 | 2479.400 | 6264.490 | 6.990 | 7.590 | 0.190 | 0.210 | 0.000627 | 0.037038 | 18.790 | 0.000 | 3.268E-05 | 19.189 |
| 3 | 265.248596 | -31.184355 | 2462.380 | 6254.420 | 8.320 | 7.510 | 0.220 | 0.210 | 0.000588 | 0.040894 | -40.540 | 0.000 | 3.216E-05 | 18.281 |
| 4 | 265.247742 | -31.182993 | 2500.500 | 6324.480 | 7.970 | 9.360 | 0.220 | 0.250 | 0.000445 | 0.036656 | -19.260 | 0.000 | 3.149E-05 | 14.133 |
| 5 | 265.204498 | -31.248816 | 4402.520 | 2939.440 | 5.210 | 6.910 | 0.140 | 0.180 | 0.000362 | 0.014235 | -6.510 | 0.000 | 2.417E-05 | 14.978 |
| 6 | 265.247681 | -31.184666 | 2503.480 | 6238.500 | 9.220 | 8.340 | 0.240 | 0.220 | 0.000310 | 0.026067 | -17.750 | 0.000 | 3.100E-05 | 10.002 |
| 7 | 265.263550 | -31.178282 | 1804.510 | 6566.500 | 4.910 | 5.520 | 0.130 | 0.130 | 0.000262 | 0.007695 | 42.930 | 0.000 | 2.444E-05 | 10.719 |
| 8 | 265.204468 | -31.246325 | 4404.470 | 3067.500 | 6.540 | 7.650 | 0.170 | 0.190 | 0.000224 | 0.012062 | -4.360 | 0.000 | 2.417E-05 | 9.269 |
| 9 | 265.195007 | -31.277824 | 4819.500 | 1447.490 | 7.670 | 6.940 | 0.190 | 0.180 | 0.000220 | 0.012632 | -11.570 | 0.000 | 2.381E-05 | 9.239 |
| 10 | 265.248749 | -31.184469 | 2456.500 | 6248.500 | 6.500 | 8.380 | 0.180 | 0.200 | 0.000203 | 0.011913 | 28.780 | 0.000 | 3.210E-05 | 6.323 |
| 11 | 265.220612 | -31.226883 | 3694.490 | 4067.500 | 7.670 | 7.030 | 0.190 | 0.180 | 0.000215 | 0.012405 | -1.100 | 0.000 | 2.416E-05 | 8.898 |
| 12 | 265.246948 | -31.184080 | 2535.500 | 6268.500 | 5.110 | 9.120 | 0.140 | 0.220 | 0.000197 | 0.009812 | -15.640 | 0.000 | 2.918E-05 | 6.751 |
| 13 | 265.223572 | -31.222876 | 3564.500 | 4273.500 | 8.120 | 9.220 | 0.220 | 0.220 | 0.000199 | 0.015933 | 39.640 | 0.000 | 2.316E-05 | 8.592 |
| 14 | 265.210846 | -31.246073 | 4123.500 | 3080.500 | 11.240 | 6.200 | 0.280 | 0.160 | 0.000199 | 0.014862 | 9.170 | 0.000 | 2.339E-05 | 8.509 |
| 15 | 265.205017 | -31.235689 | 4379.500 | 3614.500 | 8.630 | 5.100 | 0.200 | 0.140 | 0.000170 | 0.007985 | -21.260 | 0.000 | 2.508E-05 | 6.778 |
| 16 | 265.245972 | -31.203720 | 2578.500 | 5258.490 | 8.110 | 5.260 | 0.190 | 0.140 | 0.000168 | 0.007587 | 24.900 | 0.000 | 2.428E-05 | 6.919 |
| 17 | 265.203644 | -31.265575 | 4439.500 | 2077.490 | 6.330 | 6.540 | 0.160 | 0.160 | 0.000172 | 0.007552 | -39.430 | 0.000 | 2.509E-05 | 6.856 |
| 18 | 265.205444 | -31.245567 | 4361.500 | 3106.490 | 6.270 | 8.780 | 0.180 | 0.200 | 0.000170 | 0.009938 | 37.950 | 0.000 | 2.456E-05 | 6.921 |
| 19 | 265.197754 | -31.274384 | 4699.500 | 1624.500 | 7.860 | 5.500 | 0.180 | 0.160 | 0.000165 | 0.007598 | -34.390 | 0.000 | 2.469E-05 | 6.683 |
| 20 | 265.204712 | -31.248638 | 4393.500 | 2948.500 | 8.770 | 6.380 | 0.220 | 0.160 | 0.000167 | 0.009933 | -6.010 | 0.000 | 2.442E-05 | 6.839 |
| 21 | 265.246002 | -31.176868 | 2577.500 | 6639.500 | 10.480 | 6.240 | 0.250 | 0.150 | 0.000142 | 0.009743 | 1.600 | 0.000 | 2.338E-05 | 6.073 |
| 22 | 265.248993 | -31.187366 | 2445.500 | 6099.500 | 5.620 | 10.480 | 0.130 | 0.250 | 0.000141 | 0.008736 | -2.900 | 0.000 | 3.021E-05 | 4.667 |
| 23 | 265.246887 | -31.189623 | 2538.500 | 5983.500 | 4.010 | 7.000 | 0.160 | 0.110 | 0.000131 | 0.003839 | -63.780 | 0.000 | 2.676E-05 | 4.896 |
| 24 | 265.248535 | -31.178326 | 2465.500 | 6564.500 | 7.430 | 4.360 | 0.160 | 0.130 | 0.000131 | 0.004405 | -35.600 | 0.000 | 3.089E-05 | 4.240 |
| 25 | 265.246368 | -31.188768 | 2561.500 | 6027.490 | 7.410 | 10.590 | 0.220 | 0.220 | 0.000130 | 0.010655 | 42.720 | 0.000 | 2.500E-05 | 5.200 |

Clarke S. +(2019)

Evolutionary sequence for the fragmentation of high line-mass filaments



G357

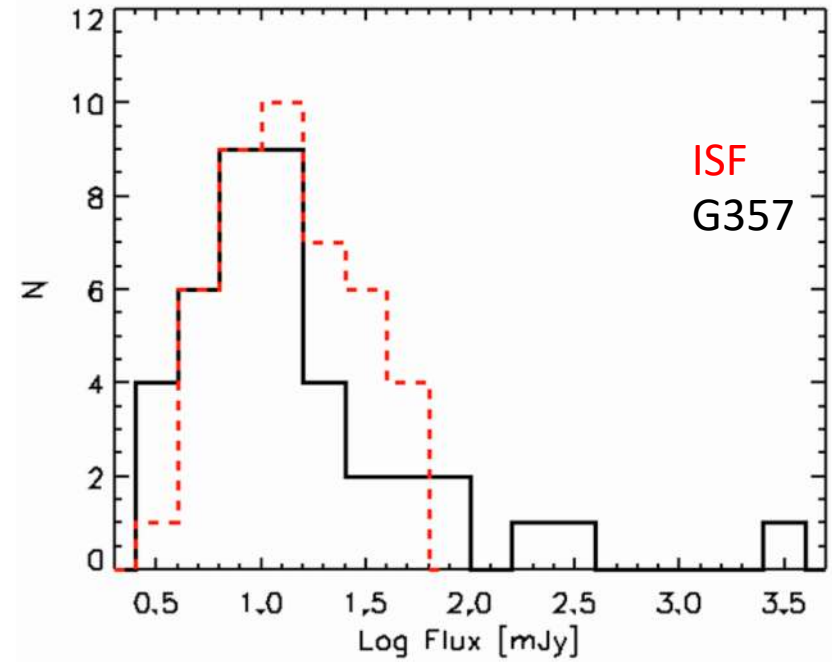
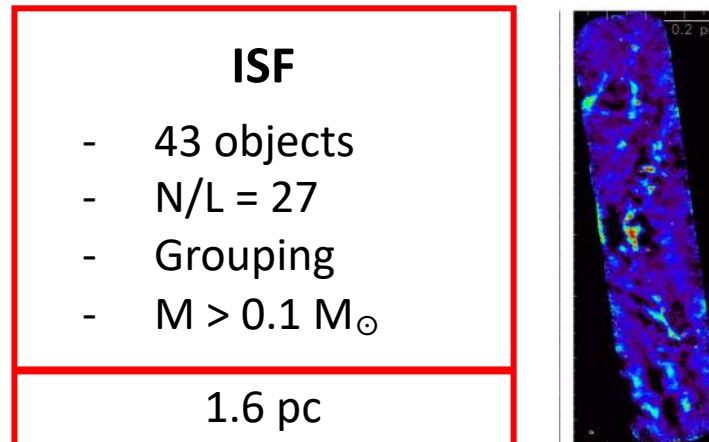
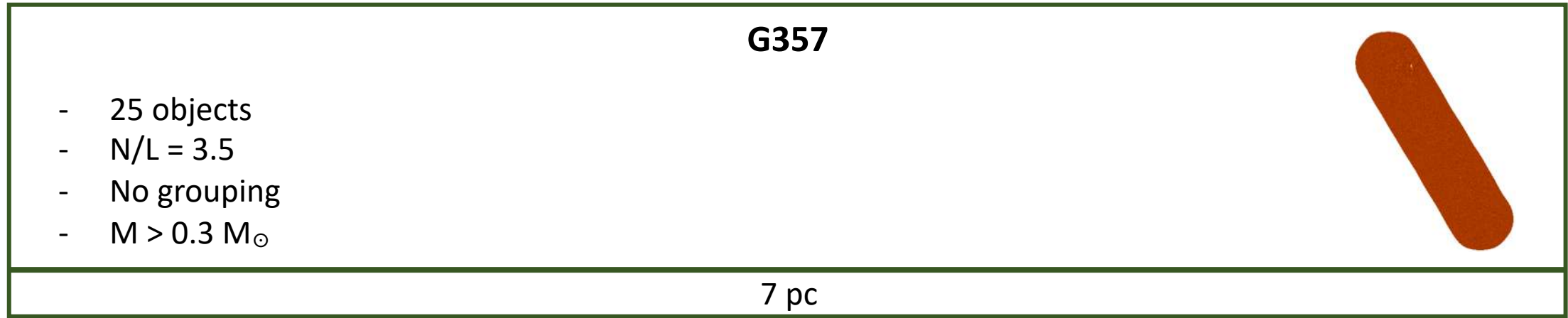
- 25 objects
- N/L = 3.5
- No grouping
- M > 0.1 M_⊙
- L = 7 pc

ISF

- 43 objects
- N/L = 27
- Grouping
- M > 0.1 M_⊙
- L = 1.6 pc

Zoom-in in the detected cores

Evolutionary sequence for the fragmentation of high line-mass filaments



Integral shaped filament (ISF) in Orion A

- **43 cores** found in ISF with **fluxes between 5 and 40 mJy** corresponding with $M = 0.1 - 2.6 M_{\odot}$
- Strong grouping where groups correspond to the gas morphology traced by the *Herschel* column density map
- Density profile along the filament show that the predictions for **Jeans' fragmentation scale is $\sim 10000 \text{AU}$** and for the filamentary **gravitational fragmentation scale is $\sim 40000 \text{AU}$** .

G357 Filament

- **25 cores** found in G357 with **fluxes between 6 and 130 mJy** corresponding with $M > 0.3 M_{\odot}$
- No grouping
- N/L smaller than in the ISF by a factor of 7
- **Complex Kinematics and velocity gradients** at the spots of the most massive clumps
- **Younger evolutionary state. It is expected to actively form stars in the future**